February, 1987

Potential Energy Surfaces for Polyatomic Reaction Dynamics

Donald G. Truhlar, *University of Minnesota - Twin Cities*
Rozeanne Steckler, *University of Minnesota - Twin Cities*
Mark S. Gordon

Potential Energy Surfaces for Polyatomic Reaction Dynamics

DONALD G. TRUHLAR* and ROZEANNE STECKLER

Department of Chemistry, University of Minnesota, Minneapolis, Minnesota 55455

MARK S. GORDON

Department of Chemistry, University of Minnesota, Minneapolis, Minnesota 55455, and Department of Chemistry, North Dakota State University, Fargo, North Dakota 58105

Received June 2, 1986 (Revised Manuscript Received July 21, 1986)

Contents

I. Introduction

The last few years have seen an explosive growth of interest in detailed studies of polyatomic reaction dynamics. Improved experimental techniques, more powerful semiclassical dynamical methods, and accurate electronic structure capabilities have all combined to focus attention on detailed dynamical questions for larger and larger systems. Many of these questions have previously been tackled primarily for atom–diatom or diatom–diatom collisions or isolated triatomics.[1-5] Although of course the final word on such simpler systems has not been said (and never will be), we will focus in the present review on more complicated cases. Thus the "polyatomic" in the title will be operationally defined to refer to a collision in which at least one collision partner or product is a triatomic or larger or to a unimolecular process involving four or more atoms. We will discuss three-atom systems briefly but only in the context of how they serve as models for larger systems. Furthermore, we will not discuss experimental results or dynamics calculations per se, but only incidentally when they are involved in the discussion of potential energy surfaces (PESs). Potential energy surfaces form the operational starting point for essentially all dynamics calculations, and—in a somewhat philosophical vein—it is sometimes stated that the determination of the PES is the goal of all experimental work (in this sense equilibrium and transition state geometries, vibrational frequencies, and barrier heights are all just aspects of the PES).

We will divide our review into two sections. In the first (section II), we will consider globally defined analytic PESs that have been constructed on the basis of electronic structure calculations, semiempirical adjustment to experimental data, or both. In the second section (section III) we consider reaction-path potentials (RPPs) based on ab initio electronic structure calculations. In each section we review a representative set of *recent* studies in the hope that this will provide an introduction to future work.

This review is limited to gas-phase reactions of nonsolvated species in the ground electronic state. (Thus, potential energy surfaces for photochemical reactions initiated by electronic excitation are not discussed.) The most recent previous reviews of gas-phase PESs for small molecules and reactions are in the book by Murrell et al.,[6] which is primarily concerned with three-body systems, but also includes a chapter on tetraatomics, and the review article by Sathyamurthy,[7] which is primarily concerned with atom–diatom and diatom–diatom systems. The review by Sathyamurthy also includes nonreactive systems, which are beyond the scope of the present review. A recently published book on chemical reaction dynamics contains one chapter on ab initio determination of PESs[8] and another devoted primarily to semiempirical PESs for atom–diatom collisions.[9]

II. Global Surfaces

A global PES is an analytic function of the internal coordinates of a system that gives the potential energy as a function of geometry. The potential energy in this context is the Born–Oppenheimer adiabatic potential for internuclear motion.[10,11] We restrict our attention here to cases where a single Born–Oppenheimer PES is sufficiently uncoupled from other surfaces that they may be ignored. We will begin with a review of some methods that have been used for three-body reactive systems, and then we will proceed to more and more complicated cases.

0009-2665/87/0787-0217$06.50/0

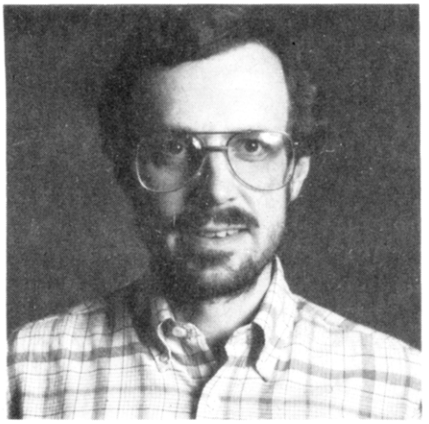

Donald G. Truhlar was born in Chicago in 1944. He received a B.A. from St. Mary's College in Winona, MN, in 1965 where his research advisers were Philip Hogan and Ernest D. Kaufman, and he completed his Ph.D. at Caltech in 1969, where his adviser was Aron Kuppermann. Since 1969 he has been on the faculty of the University of Minnesota where he is now Professor of Chemistry and Chemical Physics and Fellow of the Supercomputer Institute. He was a visiting fellow at Battelle Memorial Institute in 1973 and at the Joint Institute for Laboratory Astrophysics in 1975–76. His research interests are in theoretical chemical dynamics, molecular quantum mechanics, and electronic and molecular collision theory.

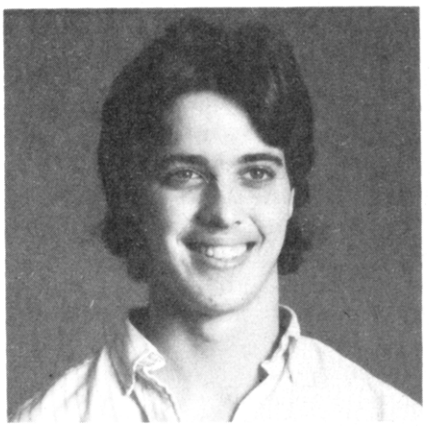

Rozeanne Steckler was born in Santa Monica, CA, in 1960. She received her B.S. degree in chemistry from the University of California at Irvine in 1982, where her research adviser was Warren Hehre. In August, 1986, she completed her Ph.D. work at the University of Minnesota under the direction of Professor Don Truhlar. The title of her thesis is "The Design of Potential Energy Surfaces for Chemical Reactions". In September she joined the Theoretical Chemistry Group at Argonne National Laboratory.

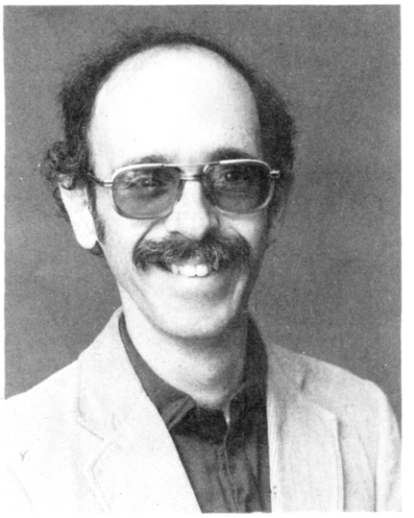

Mark S. Gordon was born in 1942 in New York City. He received a B.S. from Rensselaer Polytechnic Institute in Troy, NY, in 1963, where his research adviser was Sam Wait, and a Ph.D. from Carnegie-Mellon University, where his research adviser was John A. Pople. He was a postdoctoral associate with Klaus Ruedenberg in 1967–1970, after which he joined the faculty of North Dakota State University, where he is now professor and chairman. His research interests are ab initio molecular orbital calculations; potential energy surfaces and dynamics of photochemical processes, isomerization, and insertion reactions; and organosilicon reactive intermediates and organophosphorus chemistry.

A. Three-Atom Systems

A wide variety of methods has been used to calculate, model, and represent PESs for atom–diatom reactions. A review of these approaches is appropriate here because in many cases one or a combination of these methods can be generalized to handle polyatomic systems. We limit our discussion here to recent developments and approaches that may be useful for work on the potential energy surfaces for polyatomics. The references in this section are illustrative, not exhaustive.

Perhaps the most straightforward approach to make a PES is to perform a large number of electronic structure calculations and fit the results by least squares. An early example of a surface of this type was provided by Polanyi and Schreiber[12] who presented a fit to the ab initio calculations performed by Bender et al.[13a] for the reaction $F + H_2 \rightarrow HF + H$. (A review of the more recent ab initio results for this reaction is beyond the scope of the present review. We note, however, that these results are quite controversial because of unresolved questions about basis set completeness and the effect of higher order correlations,[13b] and this in itself is a comment on the reliability of PESs for more complicated systems.)

Another surface of this type, for the reaction $H + H_2 \rightarrow H_2 + H$, was provided by one of the authors and Horowitz, who presented a fit to the accurate ab initio calculations of Liu and Siegbahn.[14-16] This fit involves two sets of terms, the second of which vanishes for all linear geometries. In this manner the problem is separated into two steps consisting of first modeling the surface for linear geometries and then using the data for nonlinear geometries to calibrate the "bend potential". The function used to fit the surface for linear geometries is itself a sum of two terms, a London-equation term that vanishes only when one atom is infinitely removed and another term that vanishes for all linear symmetric geometries. The London equation[17] is a highly approximate form of three-orbital valence bond theory, and the London-equation term is a function of an H_2 antibonding curve that was represented by a quadratic times an exponential with parameters adjusted to the linear symmetric ab initio values for H_3. The second term of the linear potential was then adjusted to fit the rest of the linear calculations. The bend potential was successfully fit by using a sum of five additional potential functions, each of which was designed to allow flexibility for a particular aspect of the surface. This strategy of fitting a subset of the ab initio data and then adding terms that vanish for the corresponding subset of geometries can be useful in general in cases where special features are needed in

localized regions of a PES, but care must be exercised to ensure that the various localized functions join smoothly with continuous derivatives with the rest of the surface. More recently Varandas et al.[18] have refit the H_3 potential energy surface to a functional form that has the correct analytic structure for expansions about the D_{3h} conical intersection. This allows the ground-electronic-state potential energy surface to be analytically continued to yield the first excited-electronic-state surface, which is the second Riemann sheet of the same analytic function.

A third reaction for which ab initio PES data have been calculated and fit is $O(^3P) + H_2 \rightarrow OH + H$.[19-25] Two independent sets of ab initio calculations were performed and fit separately. The first fit, by Schinke and Lester[20] and based upon the calculations of Howard et al.,[19] is a 56-parameter least-squares fit to a sum of Morse functions and a three-body term that consists mainly of a polynomial of up to sixth order in all three variables multipled by a hyperbolic tangent switching function to attenuate the polynomial. The second fit, by Schatz et al.,[22] is a fit of calculations by Walch et al.[21] to a rotated Morse oscillator spline function. This second $O + H_2$ surface is of special note in that the calculations were done with the fitting function in mind. Thus, the geometries for which ab initio calculations were performed were chosen in a systematic way especially to aid in the fitting process. Later, ab initio calculations were reported[21,23,24] for the two bend potentials that give the change in energy when linear OH_2 in the degenerate $^3\Pi$ state is bent, thereby splitting the degeneracy. These bend potentials were fit to global forms by Garrett and one of the authors.[25] Although the resulting potential is well defined globally, it is designed to be most accurate in the vicinity of the variational transition state, whose approximate location was ascertained beforehand by calculations based on an earlier version of the surface. As we consider more and more complicated systems in the future, this kind of preliminary study to determine the critical configurations will become increasingly important.

Another system treated similarly is $Cl + HCl' \rightarrow HCl + Cl'$ where the apostrophe denotes isotopic substitution. In this case, ab initio calculations and a fit were reported by Garrett et al.[26] This surface consists of a rotated-Morse-oscillator spline fit for collinear geometries plus an analytic bend potential. In this case additional calculations were performed, and the final fit was carried out after dynamical calculations (based on variational-transition-state theory) on a preliminary fit gave an indication of which regions of the surface were critical.

The use of one-, two-, and three-dimensional spline fits of ab initio data was systematically investigated by Sathyamurthy et al.[27,28] They presented the first full 3D cubic spline fit to a triatomic surface, and they presented a two-dimensional cubic spline fit of the SCF calculations of Brown and Hayes[29] for $He + H_2^+$.

Ab initio surfaces have also been computed and fit for three systems involving the more ionic reactant HF, namely Li + HF,[30-33] Be + HF,[34,35a] and Ca + HF.[35b] The ab initio PES data[30] for the first of these systems was least-squares fit[31] to a many-body expansion potential in which the three-body term was varied. Further studies of this fit by Alvariño et al.[32] have shown that there is spurious structure outside the regions where ab initio values had been calculated, including a barrier in the entrance channel which is higher than the saddle point. In order to remedy this deficiency, Alvariño et al.[33] refit the surface using bond-order variables. Although the spurious structure was not entirely removed, its amplitude was greatly reduced. The first PES for the second system, BeHF, is a two-dimensional spline fit to 100 ab initio data points for collinear geometries.[34] The later work[35a] on BeFH is discussed below.

The final system to be mentioned in this illustrative survey of ab initio PESs for triatomic systems is HCO. For this system Bowman et al.[36] fitted 2000 ab initio calculations to localized Simons–Parr–Finlan functions[37] and then connected these functions with hyperbolic tangent switching functions. With such a localized approach to fitting the ab initio data they were able to generate a global potential that had the same stationary point properties as the ab initio calculations. In later work Bowman et al., reported a new fit to this data based on a three-dimensional spline function.[38]

In some cases there are significant differences in the dynamics for different forms of fits to the same ab initio data. Particularly instructive case studies have been presented by Raff and co-workers[39,40] and Wagner et al.[41-43]

There are two drawbacks to the scheme of first performing a large number of ab initio calculations and then fitting them. The first is that, for large systems, the size and the number of calculations necessary to characterize the entire surface is too expensive, especially when more than the reactant, product, and saddle point regions are important for the dynamics of the system. (The FH_2 reaction provides a good example of where other regions of the surface are equally important or even more important for some reaction attributes.[44]) To be sure that ab initio calculations are performed for the most important geometries may require an iterative process in which some type of dynamics calculation is done on a preliminary surface, and the results are analyzed for their sensitivity to various PES regions to determine where further calculations are most important to refine the surface. The second drawback to the general least-squares fitting of ab initio results is the difficulty of achieving a good fit unless physically motivated functional forms are used. The methods to be discussed next can provide some guidance as to these forms.

A second approach to representing PESs involves the use of semiempirical methods. Such methods use available experimental and ab initio information to calibrate functional forms based on simple valence theory or bond functions. Many of the systems mentioned above, e.g., $F + H_2$,[44-48] $H + H_2$,[49] $O + H_2$,[50,51] $Cl + HCl'$,[52] $Li + HF$,[53,54] and $Be + HF$,[55,56] have also been modeled semiempirically. One widely employed semiempirical method is diatomics-in-molecules (DIM).[57-59] In this method a valence-bond formalism is used to approximately express the potential of a polyatomic molecule in terms of information about its diatomic and atomic fragments. Last and Baer[60,61] expanded on this method by adding a three-center (3C) energy term, yielding the DIM–3C method. The additional term was required for standard DIM theory to give realistically high exchange barriers for the reactions $H + XD \rightarrow HX + D$, where X is a halogen. Another

example where the DIM method was used as the foundation for a surface which also includes more empirical terms is the surface of Viswanathan et al.[62] for SiH_2. These authors added adjustable parameters to the function used to evaluate the DIM coulomb integrals, and they also added an extra bending term to account for the fact that the H–Si–H angle is influenced by the nonbonded electrons on silicon which were omitted in their simplified DIM valence bond formalism. These last two cases provide good examples of one successful strategy for designing a PES, i.e., using a standard formulation as a starting point and then either adding additional terms or adding more flexibility to the adjustable parameters to remedy deficiencies or to improve areas of the surface shown by dynamics calculations to be important.

The DIM method is a promising one to serve as a starting point for the design of polyatomic PESs. A complete DIM surface for a reaction involving five or more atoms has not been reported yet, but Eaker and Parr[63] have obtained encouraging results that may provide a useful starting point for such cases. They showed that when the DIM method is extended to include larger valence-bond basis sets, it can successfully be used to model the ground and excited state potential energies for CH_2, CH_3, and CH_4.

Two closely related and widely used semiempirical methods are based on the Sato equation,[64-67] also called the London–Eyring–Polanyi–Sato (LEPS) equation, and the extended LEPS equation.[68] These may be considered as specialized ways to parameterize DIM theory. These equations contain "Sato parameters", which may be adjusted to give a desired surface feature, e.g., the correct saddle point height, or a desired dynamical result, such as having a calculated rate constant, energy of activation, or product vibrational distribution agree with an experimental value. A connection between some of the methods discussed so far is that when all Sato parameters are given the same value, the extended LEPS equation reduces to the original Sato equation, and when the one Sato parameter is zero, Sato's equation reduces to London's. In a similar fashion to that discussed already for the DIM method, a standard extended LEPS potential can be made more flexible by making the Sato parameters a function of any of the bond length, bond angle, or reaction path variables[44,48,69] and through the addition of "three-center" type energy terms. The success of these types of methods for atom–diatom systems suggests that this type of strategy would be a good starting place for larger polyatomic systems.

An example of the successful use of angle-dependent and distance-dependent Sato parameters is provided by the $F + H_2$ reaction.[44,48] We parametrized a series of surfaces for this reaction by using variational-transition-state-theory (VTST)[70a,b] calculations as a tool in the design. The VTST calculations were used to locate the bottleneck region of the PES—in the first case[44] an effective exit-channel barrier was involved—and angle- and bond-length-dependent Sato parameters were used to change the PES in this region while only minimally affecting other regions. This process is straightforward enough to allow an iterative approach. In a later surface,[48] the same strategy was used to make localized changes in the entrance channel. The combination of VTST and locally flexible functions works very well for atom–diatom reactions and should be a good starting point for the design of polyatomic PESs as well, but problems will probably arise since localized changes will not be as easy to design for the larger systems.

We would like to make one very important point about DIM and extended LEPS surfaces, and related approaches, to prevent possible misapplication. The point is that these methods are very sensitive to input data[49,56] and hence have no quantitative predictive value at the level of chemical accuracy. This should not be surprising because the set of valence bond configurations that underlie the practical algorithms is invariably very incomplete. Thus the real usefulness of these methods is not for predictive purposes but rather as a starting point for fitting or empirical adjustment.

An interesting example of the use of DIM-like functions for fitting is provided by the work of Chapman et al.[35] on BeFH. They calculated a 3D surface with close to 500 points. For fitting they used a DIM-like (but simplified) 2×2 function which built in the appropriate limits and added damped polynomial terms to fit the difference between the simple function and the calculated points in the interaction region. The resulting surface has interesting turns in the reaction path and a deep well for F–Be–H.

Another type of potential that has been used for reactions of the type $A + BC \rightarrow AB + C$ is the hyperbolic map function (HMF).[71,72] A HMF consists of a product of a Morse function and another function F that can be altered from system to system to better match available experimental and theoretical information. In the Morse function the depth parameter (D_M) and range parameter (β_M) are Eckart functions of the distance along a reaction path, and F is a function of the A–B–C bend angle. A further development of the HMF function leads to the rotated-Morse-curve (RMC) method employed by Wall and Porter[73] and by Connor and Bowman and their co-workers.[45,74]

A more systematic strategy for the design of PESs has been advocated by Murrell et al.[6] In this scheme the total potential is built up from a sum of the potentials of the dissociation fragments. Thus, depending on the size of the system, a sum of one-, two-, three-, and up to N-body terms are used. (To go much beyond $N = 4$ though becomes very difficult.) This method necessarily gives the correct dissociation limits, and, with the use of switching functions to turn on the necessary terms in the interaction regions, flexibility is available to adjust to other available information. This method was mentioned above for fitting ab initio data but can also be used empirically. Special caution is required to avoid spurious wells and oscillations in this approach.

The bond-energy bond-order (BEBO) method[75] (and related approximations[76-80]) should also be mentioned here. As originally formulated this set of approximations yields an expansion of the PES for an atom–diatom collision in the vicinity of a reaction path, but the BEBO method has several aspects which can be generalized to polyatomic systems. For example the vibrational force constants perpendicular to the reaction path are estimated in terms of the bond orders of the bonds being made and broken. This provides a natural way for stretch and bend restoring forces to tend to the correct limit as a bond is broken. A related approximation is to make bending force constants proportional to some power of a bond order. The BEBO method was

first extended to model a full PES by Kafri and Berry[81] for H_3; the resulting surface was in good agreement with the best ab initio surface. Later this method was further utilized by Garrett and Truhlar to calculate the PES for general H transfer reactions[82] and for bimolecular reactions involving the transfer of halogens, first row atoms, or a univalent metal.[83] If isotopic substitutions are to be considered, the potential energy surface should be defined in a mass-independent way.[84] Schatz et al. also presented another way to extend the BEBO method to model a whole potential energy surface.[85] Extension to the transfer of multivalent atoms has also been considered.[86,87]

One hopes that the considerable volume of effort that has been expended on three-body PESs, only a small fraction of which was mentioned here, will provide a solid foundation for understanding PESs of systems involving four or more atoms.

B. Four-Atom Systems

A portion of the PES for $HeH^+ + H_2 \rightarrow He + H_3^+$ was constructed by McLaughlin and Thompson,[88] who constrained the system to follow a reaction path of C_{2v} symmetry. The surface is a combination of two-dimensional and one-dimensional cubic spline fits to calculations performed by Benson and McLaughlin.[89]

An analytical polyatomic PES has been designed for the reaction $OH + H_2 \rightarrow H_2O + H$ by Schatz and Elgersma.[90] Their approach nicely illustrates how various methods can be combined to fit a many-body PES. Their surface is an empirical fit to the ab initio calculations of Walch et al.[91,92] It treats the three H atoms as distinguishable, so we label these H_a, H_b, and H_c. The fit consists of a sum of three Morse potentials, for the OH_a, H_aH_b, and H_bH_c pairs, an extended LEPS function for the OH_bH_c interaction, a Sorbie–Murrell-like three-body potential to model the quadratic force field for H_aH_bO, and a four-body correction term. The latter is a sum of two terms, each of which is a product of gaussians which depend on the OH_a, OH_c, H_aH_b, and H_aH_c bond distances. The resulting surface has a planar MEP. A defect in the surface fit is that the geometry is cis at the ab initio saddle point but trans at the saddle point of the fit surface. Rate constants calculated with this surface agree with experiment within a factor of 1.7 over the entire temperature range from 298 K to 2400 K.[93,94] Additional dynamics calculations show that this surface also explains the large rate enhancement when H_2 is vibrationally excited and the small enhancement when OH is excited.[95] In subsequent work with this surface Rashed and Brown[96] eliminated spurious wells in the asymptotic region of the surface by modifying the Morse functions for the H_aH_b and H_bH_c interactions such that they die off to zero more rapidly. Rashed and Brown achieved excellent agreement with the ab initio data for reactant and product properties, the saddle-point barrier height, and zero-point energy. However the ab initio saddle-point geometry is still not well reproduced, and the resulting surface also has problems far from the saddle point.[96] The latter problems are due in part to lack of ab initio points in the regions in question and also to the inflexibility of the functional form. This illustrates the need for functional forms that allow one to adjust selected regions of the PES without affecting (or with minimal effect on) the rest of the surface. The OH + H_2 reaction will be discussed again in section III.A. from the point of view of reaction-path potential techniques.

The method of Murrell and co-workers,[6] discussed briefly in section II.A., has been used by Carter et al. and by Halonen et al. to obtain PESs for both H_2CO[97] and C_2H_2.[98,99] For both of these systems the PES was written as a many-body expansion which includes terms for each of the one-, two-, three-, and four-body interactions. With this type of formulation each three-body term is a correction, for the energy of a triatomic subsystem, to the sum of the one- and two-body interactions, and the four-body term vanishes when any one atom is removed. One hope (as yet unrealized) with this type of formulation is that a library of these various terms can be accumulated so that the terms for a new system can be taken from this library and used with only minimal adjustments. Formaldehyde has also been extensively studied using RPP techniques; these studies will be discussed in section III.A.

The surface of Murrell and co-workers for H_2CO has been criticized by Swamy and Hase,[100] who pointed out that it does not give a good representation of the saddle point.

The surface of Halonen et al.[98] for acetylene, which is designed to be valid at all dissociation limits as well as regions close to the equilibrium geometry, was adjusted using both ab initio (self-consistent electron pairs calculations[101] using a double-zeta-plus polarization basis) and experimental information. In this case the expansion included six two-body interaction terms, one for each of the possible atomic pairs in C_2H_2, four three-body terms, two of which are for C_2H subsystems and the other two of which are for CH_2 subsystems, and a four-body term to describe the intrinsically acetylenic interactions.

Stine and Muckerman[102] presented an 8 × 8 DIM treatment of the two lowest electron states of $H_2^+ + H_2 \rightarrow H_3^+ + H$. They also discussed the charge-transfer reaction $H_2^+ + H_2 \rightarrow H_2 + H_2^+$.

Wolfsberg and co-workers have presented two PESs for NH_3.[103,104] Although the present review is not intended to cover nondissociative PESs for isolated simple (i.e., nonisomerizing) molecules, the inversion mode of NH_3 may be viewed as a prototype isomerization, and the techniques employed in their work may also be applicable to more complicated isomerizations. They started with a quadratic–cubic–quartic expansion about the equilibrium point and replaced the potential in the wide-amplitude inversion mode by a globally defined term with a double-minimum character. Brown et al.[105] have used these surfaces to study the rate of interconversion of the ammonia invertomers and the magnitude of the tunneling splitting of the energy levels. Another simple isomerization system which has been treated similarly is the hydrogen-bond switching reaction HF···HF → FH···FH. Hancock et al.[106] calculated the tunneling splitting due to this degenerate rearrangement with a PES by Barton and Howard.[107] This surface treats each HF molecule as a rigid rotor. A later surface by Michael et al.,[108] which was fit to coupled-cluster ab initio calculations, includes the HF stretches but is restricted to planar geometries.

In early work, Raff[109] developed a general potential for four-body systems of the type A + BCD → AB +

CD. Specifically, Raff was concerned with the reaction $K + C_2H_5I \rightarrow KI + C_2H_5$ where the C_2H_5 radical was approximated as two bricks, one with mass 14 u and the other with mass 15 u. (*Note:* 1 u = 1 *atomic mass unit.*) This surface was based on a three-body surface for $K + CH_3I \rightarrow KI + CH_3$ by Bunker and Blais[110] as modified by Karplus and Raff.[111,112] The three-atom potential is a sum of two Morse potentials and an attenuated exponential. Raff added a Morse potential to this to describe the CH_3–CH_2 interaction and an exponential function for the repulsion between K and the center of mass of the C_2H_5 group.

C. Five-Atom Systems

The PES for $O_3 + NO$ has been modeled by both Chapman[113] and Viswanathan and Raff.[114] This system is particularly complex in that a variety of excited-state NO_2 products can be formed. In each of the two studies more than one surface was developed in an attempt to understand the system better. In the first case, Chapman[113] developed two potential functions, one for the reaction in which an oxygen is abstracted from either end of O_3 and one for the abstraction of the middle oxygen. Both of these functions have the same basic form, namely, they consist of a sum of Morse functions to model the stretches, functions of cosines of the angles for the bend potential, and pairwise nonbonding repulsive interaction terms for nonbonding atoms. With each of these functions Chapman calibrated several surfaces representing various electronic states of NO_2 and various classical barrier geometries. For the surfaces representing the abstraction of one of the end oxygen atoms, the classical barrier height was kept at 3.5 kcal/mol, while for the surfaces representing abstraction of the middle oxygen the barrier height is 3.0 kcal/mol.

The second study of $O_3 + NO$, by Viswanathan and Raff,[114] concentrated on the abstraction of a center oxygen in O_3 to form two of the possible electronic states of NO_2. The various surfaces they calibrated were designed to study the effect of barrier height and location on the dynamics of the system. These surfaces were built from the following terms: two three-body LEPS-type potentials for the interaction of the nitrogen with two oxygen atoms of O_3, a three-body interaction potential for O_3, and various two-body interactions and angle-dependent terms. Viswanathan and Raff generated five PESs, four of which have identical barrier locations but different barrier heights, and the fifth of which has a different barrier location. They found that the best agreement with experimental reaction cross sections occurred when they performed classical trajectory calculations on the fifth surface which has a barrier height of 3.5 kcal/mol.

As is typical of many of the surfaces discussed in this review, it is not known whether any of the $O_3 + NO$ surfaces is qualitatively correct.

Recently Duchovic et al.[115] have designed an analytic polyatomic PES for the dissociation of methane. The method they used is both very general and very complex in terms of the fitting function used. In the formalism they used, the potential is written as a sum of Morse potentials for the stretches and a sum of Taylor series expansions for the various bends. These potentials are optimized using a least-squares fit to ab initio data and available spectroscopic information. A nice feature of this approach is that the necessary symmetry can be built in such that for methane all hydrogens are equivalent. In section III.C. further studies of the dissociation of methane using reaction-path potentials are discussed.

A PES for another dissociation reaction, $SiH_4 \rightarrow SiH_2 + H_2$, has been designed by Viswanathan et al.[116] In this case the potential function is composed of a sum of Morse functions plus a sum of six harmonic terms to model the bending potentials. Switching functions are used to attenuate the various Morse functions. A major flaw in the surface is the discontinuity in the first derivatives at equilibrium SiH_4. This kind of problem can occur whenever a potential is attenuated by using a variable like the longest bond length if one is not careful to explicitly ensure continuous derivatives at the point where two bond lengths switch. We recommend that potential builders go farther than guaranteeing continuous first derivatives. The potential should be continuous through second derivatives if it is to be used to generate a harmonic reaction-path potential, and it should be continuous through fourth derivatives if it is to be used for an anharmonic reaction-path potential, calculations of the vibrational mode couplings, or calculations of reaction-path curvature components. The IRC for this system is discussed in section III.C.

McDonald and Marcus[117] presented four model surfaces, loosely representing CH_4 and CH_3Cl, and used them to study intramolecular energy redistribution in unimolecular processes. The analytic form used is flexible enough to have or not have a barrier to dissociation and to have or not have a coupling between the dissociating bond and the spectator bonds.

D. Six-Atom Systems

A limited number of PESs have been designed for reactive polyatomic systems with six atoms.[118–124a] For systems of this size the number of dimensions and possible reactions involved make it very difficult for surface builders to treat the entire surface with equal attention. A generally appealing approach in such a case is to concentrate on obtaining an accurate model for the reactants, products, and saddle point for the reaction of interest and then as accurately and smoothly as possible to connect up these regions to give a surface upon which the dynamics can be studied. Then, as information accumulates about the relation of the dynamics to PES features, one can attempt to improve the surface at specific intermediate geometries.

The first six-atom PES to become available was that designed by Bunker and Pattengill[118] for CH_5. This surface was restricted to the abstraction reaction, e.g., $T + CH_4 \leftrightarrow HT + CH_3$, by the limitation that only one methane hydrogen was treated as reactive. The authors found that this limitation gave an unrealistic surface. This surface was improved by Valencich and Bunker[119,120] so that the substitution channel, e.g., $T + CH_4 \leftrightarrow H + CH_3T$, is present. Further minor modifications were made by Chapman and Bunker.[121] The final surface consists of a sum of Morse functions for various bonds, a specialized abstraction channel potential, a hydrogen repulsion term, and another function to give

the desired H–C–H bond angles throughout the reaction. The additional term is the product of two switching functions and a tabular function, summed over H–C–H bond angles. The Morse depth parameters are also tabular. The main problem with this approach is that with tabular functions a whole new set of values has to be computed for each system to be modeled, whereas for analytic functions the goal is to be able to adjust a minimal number of parameters for each new system. With tabular functions one cannot easily build upon past experience to design a new PES. Another drawback to this type of scheme for angular adjustments is that numerical difficulties can occur in interpolating between the tabular points as required to compute gradients and a RPP, especially if the spacing between the tabular points is much larger than the step size used in following the gradient.

An apparent problem with the surfaces of Bunker and co-workers for CH_3–H′–H″ is that the C–H′–H″ part of the potential yields an MEP that "cuts the corner" more than the MEP's obtained by semiempirical valence-bond theory, BEBO, or fits to ab initio calculations. This leads to a lower maximum value of the reaction-path curvature. This apparent defect is also present in the HMF function used by Bunker and co-workers for A + BC reactions (see section II.A.). For CH_3–H′–H″, the C–H′ and H′–H″ distances at the saddle point on the Valencich–Bunker–Chapman (VBC) surface are both larger than the best ab initio estimates,[124b] indicating that the VBC saddle point is not so much "earlier" or "later" than the ab initio one, but rather "farther out".

At about the same time as the VBC surface was created Raff[122] also designed a PES for both the exchange and abstraction channels of T + CH_4. This potential is a sum of four three-body terms and an angle-dependent term to control the change of geometry from tetrahedral CH_4 to trigonal planar CH_3. This approach converts a six-body surface into a sum of potentials like those that have been modeled successfully for atom–diatom reactions. Since Raff used functions similar to the extended LEPS function to model each of the three-body interaction terms, additional flexibility could be built into his surface using techniques similar to those discussed above, although Raff did not do this. The method used by Raff is not applicable to systems for which three-body interaction terms do not correctly describe all the significant interactions involved, but it is a legitimate approach for CH_5 since the hydrogens on the methyl group are mainly spectator atoms. The major problem with this type of surface is that, as in most approaches, the adjustable parameters must be chosen with caution in order to get a realistic representation of the saddle point.

A more specific problem with the formulation as given by Raff is that the first derivatives are discontinuous just as in the SiH_4 PES discussed above. As in that case, the CH_5 PES involves a variable, R^+ (the largest C–H bond length in methane), which gives a discontinuity at equilibrium methane. In his CH_5 PES Raff also uses a switching mechanism to change the bond angles from tetrahedral methane to planar methyl. The formulation seems reasonable except that the derivatives are discontinuous at the switching points. These problems are not insurmountable, but they show that one must be careful when designing switching functions for PESs to insure that the surface is smooth and continuous everywhere.

TABLE I. Saddle-Point Characteristics for $CH_3 + H_2 \rightarrow CH_4 + H$

	PolCI	VBC	Raff
R_{C-H}, a_0	2.04	2.07	2.07
R_{C-H_a}, a_0	2.78	3.48	3.04
$R_{H_a-H_b}$, a_0	1.74	1.71	1.48
$\nu^\ddagger$, cm^{-1}	$974i$	3672^i	1478^i

An important consideration to keep in mind when using sums of atom–diatom potentials, e.g., rotated Morse or extended LEPS functions, is that any flaw in the atom–diatom PES is most likely going to be present in the polyatomic PES. Since Valencich, Bunker, and Chapman[119–121] and Raff[122] modeled the PES for the same CH_5 system but used different atom–diatom potentials, it is instructive to see the effect of the choice of the HMF atom–diatom potential by VBC and the modified LEPS potential by Raff. Both surfaces can be judged by comparison to the PolCI calculations of Walch et al.[124b,125] Table I gives the saddle-point characteristics for the PolCI calculations, the VBC surface, and the Raff surface. The labeling convention we use is $CH_3 + H_aH_b \rightarrow CH_3H_a + H_b$; R_{x-y} is the x–y internuclear distance, and $\nu^\ddagger$ is the imaginary frequency of the unbound normal mode at the saddle point. (In order to locate the saddle point on the VBC surface we had to make some minor modifications to the surface to correct discontinuities in the second derivatives. A complete description of the modifications made and a more detailed analysis of the saddle point and other features of this surface and the Raff surface is available elsewhere.[126]) The first three rows of Table I give the saddle-point geometry, showing that the Raff and PolCI saddle points are similar except that the Raff one occurs earlier. As discussed above, the VBC saddle point occurs in a different region. The last row of this table shows the imaginary frequency for these three saddle points, which characterizes the width of the barrier near its top. The VBC surface has an imaginary frequency that is over three times the value computed in the PolCI calculations, and as such has a barrier that is much thinner than the Raff surface. This stresses the importance of using physically realistic fitting forms. Even if the barrier on the VBC surface were raised, the amount of tunneling that would be present would be so unrealistic that the surface would not give meaningful results in dynamics studies. Various reaction-path-potential studies have also been carried out for the CH_5 system, and they are discussed in section III.D.

Bunker and Goring-Simpson[124a] have developed a general six-atom empirical potential energy surface for M + $CH_3I \rightarrow MI + CH_3$ reactions where M is an alkali. Their potential consists of a three-body interaction term for the alkali–I–CH_3 interaction, a three-body hydrogen interaction term (the same as used by Bunker and co-workers for CH_5) that controls the geometry change of the methyl moiety, and an alkali–hydrogen repulsion term. The potential is written in terms of various general parameters which they then adjusted for the reaction Rb + CH_3I using molecular beam data.

Another six-atom PES that has been studied is that for the isomerization reaction $CH_3NC \leftrightarrow CH_3CN$, which

was modeled by Bunker and Hase.[123] Several surfaces were designed, the basic form being a sum of Morse functions and harmonic potentials. They added quartic anharmonicity and torsional terms to the basic form.

E. Seven-Atom and Eight-Atom Systems

Bunker and Hase and their co-workers also designed PESs for the hydrocarbons C_2H_5[127] and C_2H_6[128] by using similar techniques to those mentioned above for CH_3-NC. An example of this approach is provided by the surface of Sloane and Hase[129] for $C_2H_5 \rightleftarrows H + C_2H_4$. The analytic surfaces Hase and co-workers have constructed both for this reaction and for $CH_4 \rightarrow CH_3 + H$ (discussed above) use BEBO ideas. For the C_2H_5 surface the procedure employed was to connect the saddle-point region, whose properties were computed using single-configuration SCF calculations, to the product region whose properties are known from a combination of calculations and experiment. This was accomplished by expressing the potential energy along the reaction path as a sum of four terms. This work was later extended to the chemical reaction $F + C_2H_4 \rightarrow H + C_2H_3F$ by Hase and Bhalla.[130] These workers found that the previous surface for ethylene could be used as a starting point by considering the reaction to occur in two stages, $F + C_2H_4 \rightarrow C_2H_4F \rightarrow H + C_2H_3F$, and using a separate surface for each. Only slight modifications of the previous surface were necessary to substitute a fluorine atom for a hydrogen atom. In employing this procedure care must be taken such that the joining of the two surfaces occurs smoothly.

F. Ten-Atom and Larger Systems

An important general step in creating PESs for polyatomic systems is the modeling of internal vibrations. One example of success in this area is the modeling of the vibrations of benzene. Hase and co-workers found that the vibrations in benzene could be modeled by attenuating the force constants in the various H–C–C bends.[115,127,131-133] Benzene vibrations have also been studied by Sibert et al.[134,135] In another interesting study on a hydrocarbon, Steele showed that the torsional potential of *n*-butane can be calculated by a small-basis-set ab initio method, and little accuracy is lost if this is carried out with fixed C–H bond lengths and bond angles.[136]

Parts of potential energy surfaces have been modeled for even larger systems using similar techniques as well as more specialized ones that are often discussed under the general heading of "molecular mechanics".[137-150] For example, substituent effects on internal rotation barriers have been studied widely and a systematic store of information is available.[139,140] For constructing potential energy surfaces of reactive systems though we require information about how such barriers depend on large-amplitude extensions of bond lengths, and there is much less information available on this topic. Recently Singh and Kollman[151] have presented a technique for treating the reactive part of a molecule by quantum-mechanical-electronic-structure techniques and the nonreactive or spectator part by molecular mechanics. Further applications and refinements of such methods could be very useful for modeling multidimensional potential energy surfaces of reactive systems. A difficulty, however, in using the molecular mechanics parameterizations for reactive potential energy surfaces is that the former were not usually intended by their original authors to deal with the very wide-amplitude distortions that must be considered in reactive systems.

Although the goal of this review, as stated above, is to consider potential energy surfaces for intramolecular and intermolecular interactions in reactive systems, we should keep in mind that most degrees of freedom in larger systems are nonreactive. Hence techniques for studying intermolecular interactions in nonreactive systems can provide a valuable starting point for modeling these degrees of freedom. This is too large a field to review completely here, but we mention two approaches. One is the multiproperty empirical fitting of multiparameter empirical forms. A good example is the He–CO_2 potential of Keil and Parker.[152] In this potential CO_2 is treated as rigid, and the goal is to obtain the radial and angular parts of its interaction energy with He. For this purpose an empirical potential is simultaneously fit to nine different types of experimental data. Although the resulting potential is not transferable, it could be used to test transferable models. A second general approach not mentioned yet is the electrostatic model.[153-156] Electrostatic models can be made very systematic, and there is a large body of literature delineating their successes and failures and sometimes proposing extensions. Like the intramolecular molecular mechanics models though, this technique requires further development to be used in conjunction with other methods for reactive degrees of freedom.

III. Reaction-Path Potentials

The previous section considered global representations of potential energy surfaces, sometimes with empirically adjusted parameters and frequently based on ab initio calculations or aided by them at key points on the surface. Ideally, when using electronic structure calculations to compute potential energy surfaces, one would use them to calculate the *entire* surface. Unfortunately the expense for such an undertaking is usually prohibitive. In many cases though, where the calculation of a full surface is impractical, it *is* possible to calculate the minimum energy path (MEP) connecting a particular set of reactants and products and passing through the classical transition state. Several authors[157-164] have noted that a particularly convenient definition for the MEP is the union of a path starting at the saddle point and following the steepest descents curve through mass-scaled or mass-weighted coordinates to products with another such path from the saddle point to reactants. The appropriate mass scaling for a cartesian coordinate of an atom of mass m_A is any constant proportional to $\sqrt{m_A}$. In quoting numerical results below, we will evaluate $\sqrt{m_A}$ in atomic mass units (u), resulting in a mass-weighted reaction coordinate with units of $u^{1/2}$Å or $u^{1/2}a_0$. Generalizations to reactions with zero or two or more saddle points are available.[26,70b,165,166] The reason for using mass-weighted coordinates is that the same reduced mass factor appears in front of every squared momentum term in the Hamiltonian, i.e., the coordinates are "isoinertial". The

use of mass-scaled coordinates also has the consequence that each downhill segment of the MEP corresponds to an infinitely damped classical trajectory along which an infinite frictional force continuously damps the local kinetic energy to zero.[164] The MEP defined this way has been termed the intrinsic reaction coordinate (IRC) by Fukui and co-workers,[161-163] and we will use the terms interchangeably.

Simple methods for determining an approximate MEP include the linear least motion[167,168] (also called linear synchronous transit) and distinguished-coordinate[169-171] approaches. Both methods are often used as the inital stage in a saddle point search, but may also be considered as reaction paths in their own right. In the former one connects reactants with products by using a grid of linearly interpolated points, while in the latter one chooses a "distinguished coordinate", usually a bond length, bond angle, or dihedral angle, and allows all other coordinates to adjust as the reaction coordinate is varied from its value at reactants to that at products. A difficulty with both of these reaction paths is that, except for the simplest reactions, they are not guaranteed to pass through the transition state, nor will they necessarily correspond to the correct minimum-energy path. The linear-least-motion method also suffers from an ambiguity in the definition of reactants or products when applied to bimolecular or dissociation reactions. The distinguished-coordinate approach may lead to a reaction path that is not smooth.

The systematic starting point for a calculation of the full MEP is the determination of the transition state or saddle point for the reaction of interest. Several approaches are available for locating stationary points.[167-185] The most effective of these rely on knowledge of at least the first derivatives of the energy with respect to $3N$ cartesian or $3N - 6$ internal coordinates for an N atom system. These first derivatives supply the information necessary to determine the geometry corresponding to a minimum norm of the gradient, which is one condition for a saddle point. A second criterion for a saddle point is the existence of one (and only one) negative eigenvalue of the force constant matrix at the saddle point; thus the availability of the second derivatives of the energy is important as well. The second derivatives are also helpful in providing initial search directions[182,183] and are required at several points along the minimum-energy path if one is to use the MEP as the starting point for a reaction-path potential[70b,82,157,158,160,186-189] or a variational transition-state-theory calculation. Evaluation of the leading terms in the anharmonicity or of matrix elements that couple different vibrational modes and allow energy transfer between them requires third derivatives of the energy.[70b,188-190] Thus, the availability of analytical expressions and algorithms for energy derivatives are necessary both for the efficient and accurate determination of MEPs and also for their use in dynamical calculations. Algorithms that generate energy derivatives as well as energies from electronic structure calculations are now *routinely* available for both first and second derivatives of restricted closed-shell Hartree–Fock (RHF)[167,191] and unrestricted Hartree–Fock (UHF)[192] wave functions and for first derivatives of multiconfigurational self-consistent-field (MSCSF)[193,194] and restricted open-shell Hartree–Fock (ROHF) wave functions.[195] Analytical expressions for second derivatives for the latter two types of wave functions[196] and for configuration-interaction (CI) wave functions[197,198] have also been developed, as have the third derivative expressions for RHF and UHF wave functions.[199] The corresponding first derivatives for RHF, UHF, and MCSCF wave functions based on pseudopotentials are also available.[200] Very recently a computational procedure was proposed for gradient calculations based on multireference configuration interaction (MRCI) wave functions.[201] These developments are expected to play an increasingly important role in facilitating the interfacing of ab initio electronic structure calculations with modern theories for the prediction of reaction rates.

Once the saddle point for a reaction has been found, the next step in calculating a reaction-path potential is to determine the minimum-energy path. The most straightforward approach is simply to follow the mass-scaled steepest descent path by successively generating the gradient in mass-weighted cartesian coordinates and making a small move in the negative of this direction. Truhlar et al.[190] have demonstrated the necessity of using small (0.001–0.05 a_0) step sizes in the negative gradient direction in order to ensure that one remains on the true MEP in this numerical procedure. Of course, the smaller the step size, the more costly the calculations become; thus some efforts have been undertaken to obtain more accurate results with larger steps by attempting to correct for possible deviations from the path in such steps. Ishida, Morokuma, and Komornicki,[202] for example, demonstrated that the minimum-energy point along a line bisecting two successive gradient vectors on the numerically determined steepest descent path will be closer to the correct MEP than a point obtained from the simple negative gradient following (Euler) procedure. Schmidt, Gordon, and Dupuis[203] suggested a method for making this interpolation procedure more efficient by reducing the number of function evaluations required. An important question with regard to such schemes is whether the computer time required to carry out the interpolation (or extrapolation) technique is greater or smaller than that which is saved by allowing larger step sizes. This question is currently being addressed in this laboratory[204] by a systematic analysis of the accuracy of predicted rate constants as a function of step size and by employing various improved procedures for integrating the differential equation that yields the MEP.

Once the minimum-energy path has been determined, either qualitative or quantitative investigations of the reaction dynamics can be carried out. The general approach to be taken in the remainder of this section will be to consider in turn each of the reactions whose MEP has been studied and to discuss the calculations leading to this MEP and related theoretical developments for the reactions so studied. For background on the use of the MEP in dynamics calculations, the reader is referred to a series of papers on dynamics, including generalized-transition-state theory, in terms of reaction-path Hamiltonians (RPH) by Miller and co-workers[188,189] and by Truhlar and co-workers (ref 25, 26, 44, 47, 48, 70a,b, 82, 93–95, 126, 160, 165, 166, 190, 205–211). These papers also contain references to related work by other groups.

Generalized-transition-state theory, including the special case of variational-transition-state theory, pro-

vides a systematic means to improve on conventional-transition-state theory and also to extend it to reactions of vibrationally excited species. A fundamental aspect of the theory is that it attempts to estimate the location and properties of true dynamical bottlenecks, e.g., free energy maxima, without assuming that they are located at the saddle point. In the work of Truhlar and co-workers the search for the true multidimensional dynamical bottlenecks is made practical by examining a sequence of trial bottlenecks parameterized by their location along the one-dimensional MEP. Interpolation models[210] have been developed to reduce the number of ab initio energy functions and derivatives that are required. Tunneling contributions may be included by multidimensional approximations that take account of the curved nature of the MEP in mass-scaled coordinates. For small curvature of the MEP it is sufficient to know the MEP and the potential in its vicinity to perform such calculations,[70b,211] but for large reaction-path curvature one must know a wider swath.[26,70b,190,211-215] Two quantities that play important roles in variational-transition-state theory and in multidimensional-tunneling calculations are the vibrationally adiabatic ground-state (VAG) potential curve and the reaction-path curvature. The vibrationally adiabatic potential curve is defined as

$$V_a^G(s) = V_{MEP}(s) + \epsilon^G(s) \quad (1)$$

or

$$\Delta V_a^G(s) = V_a^G(s) - V_a^{RG} \quad (2)$$

Here s and $V_{MEP}(s)$ are the distance and Born–Oppenheimer potential, respectively, measured along the MEP, $\epsilon^G(s)$ is the local zero point energy of the bound vibrational modes along the MEP, and V_a^{RG} is the reactant value of $V_a^G(s)$. It is conventional to take $V_{MEP}(s) = 0$ at reactants, in which case V_a^{RG} becomes the reactant zero-point energy. Within an additive constant, $V_a^G(s)$ is the generalized free energy of activation at 0 K, and its maximum determines the location of the variational transition state at 0 K. The calculation of either the vibrationally adiabatic potential curve or the generalized free energy of activation requires the calculation of generalized normal mode frequencies for the vibrational modes orthogonal to the reaction path and, optionally, anharmonic force constants for these modes. The reaction-path curvature is a scalar for collinear three-atom systems and a vector in other cases. The components of this vector along the generalized normal modes are called $B_{mF}(s)$, where m denotes a particular normal mode and F denotes the reaction coordinate, and the magnitude of the curvature is

$$\kappa(s) = \{\sum_{m=1}^{F-1} [B_{mF}(s)]^2\}^{1/2} \quad (3)$$

where $F = 3N - 6$ for nonlinear reaction paths and $3N - 5$ for linear paths. Because reaction-path curvature plays an important role in dynamics calculations based on RPP's or RPH's, we shall reserve the word "curvature" for curvature of the reaction path. Use of the word "curvature" to refer to the second derivative of the potential can be confused with references to reaction-path curvature and hence is discouraged.

The same quantities also occur in Rice–Ramsperger–Kassel–Marcus (RRKM) theory, which, for the purposes of this review, may be considered simply to be the special case of transition-state theory for a unimolecular reaction.[216,217] More general dynamical procedures employing MEP-based descriptions of the system, including $V_a^G(s)$, have been considered by Miller and co-workers.[188,189]

Even when full dynamics calculations are not performed, much can be learned by studying the vibrational frequencies and the geometrical changes along the MEP, or by just studying the MEP and its curvature.[187,218-220] An even simplier way to combine electronic structure calculations with dynamics is to use conventional-transition-state theory to predict reaction rate constants, perhaps incorporating simple models for tunneling corrections. These calculations require at most the determination of structures, energies, and first and second energy derivatives for reactants, products, and saddle point, and they will not be reviewed here. Several papers have described the evaluation of the minimum-energy paths for the purpose of qualitative descriptions of either bond breaking and forming processes or reaction dynamics. These applications do not require evaluation of the second derivative matrix at points other than the transition state, and they will not be exhaustively reviewed here. Nonetheless, because such calculations are the first step in the predictions of reaction rates and because they can provide some insight into reaction dynamics, several of them will be mentioned briefly in the following discussion.

Because electronic structure calculations play a large role in this section and because such calculations may be performed at a variety of levels, we conclude this introduction by quickly reviewing the electronic structure methodologies to be mentioned below. Rather than give an exhaustive list of basis sets and computational methods, this review will be limited to those approaches which have been used in the papers to be discussed below.

With the exception of a few semiempirical potential-energy surfaces, based on variants of CNDO[221] or MINDO,[222] most of the calculations to be discussed have used ab initio wave functions with gaussian basis sets. The types of basis sets used include minimal, double zeta, split valence, and extensive basis sets. In minimal basis sets the number of gaussian subshells employed for each atom equals the number of occupied or partially occupied subshells in the free atom. The most commonly used minimal basis set is STO-3G,[223] in which a Slater type function is approximated by a linear combination of three gaussians. In double zeta (DZ) basis sets, each minimal basis function is replaced by two functions, one with a smaller and one with a larger exponential parameter. The most commonly used DZ basis sets are those developed by the groups of Huzinaga[224] and Dunning.[225,226] Split-valence basis sets, primarily developed by Pople and co-workers, are double zeta for the valence shells and minimal for the inner shells. The most common notation for split valence basis sets is N-M1G. This means that each inner shell basis function is expanded in N gaussians, each inner valence basis function is expanded in M gaussians, and each outer valence basis function is represented by a single gaussian, where inner and outer refer to the spatial extent of the basis function. Using this notation, the most popular basis sets of this type have been 3-

21G,[227] 4-31G,[228] and 6-31G.[229] Extensions of the foregoing, such as triple zeta (TZ), are obvious. For the atoms in the first two periods of the periodic table, a triple split-valence basis set, 6-311G,[230] has been developed. In polarized basis sets, one adds atomic symmetry types to the basis set that are unnecessary for the description of the ground-state atomic electronic structure at the Hartree–Fock level but allow for the polarization of the local electron density when an atom is placed in the vicinity of another (polarizing) atom. In simplest terms, this corresponds to adding functions with the next higher l quantum number to an atom (p functions on hydrogen, d functions on carbon or silicon, for example). Normally, polarization functions are added only to basis sets of split valence or double zeta quality or higher, so common notations are, for example, DZP and TZP for double zeta or triple zeta plus polarization. For the split-valence basis sets the types of polarization functions are indicated in parentheses, with the heavy atoms appearing first. Thus, 6-311G(d,2p) indicates that the 6-311G basis set has been augmented by a set of d functions on each non-hydrogen and two sets of p functions on each hydrogen.[231] (An older notation used one or more asterisks to denote added polarization functions.) It is also often necessary to add basis functions which are more diffuse (that is, have smaller exponents) than those ordinarily present in a doubly or triply split basis set. Such functions are denoted by a + for heavy atoms and a ++ if they have been added to hydrogen atoms as well. Thus, the ++ in 6-311++G(d,2p) suggests that a set of s and p diffuse functions has been added to the basis for each heavy atom, and a set of diffuse s functions has been added to each hydrogen.[232]

Once the one-electron basis set is chosen, one must consider the form of the many-electron wave function. The simplest general procedure is the single-configuration self-consistent-field method (SCF), including the special cases of restricted Hartree–Fock (RHF),[233] in which all spatial orbitals are doubly occupied, unrestricted Hartree–Fock (UHF),[234] in which different orbitals are used for different spins, and restricted open-shell Hartree–Fock (ROHF),[235-237] in which some orbitals are doubly occupied and some are singly occupied. However to obtain a realistic potential energy surface, it is generally necessary to go beyond the single-configuration SCF approximation in order to approximate at least part of the correlation energy.

The two general methods used to include correlation energy are based on the variational principle and perturbation theory. The first of these includes conventional configuration interaction (CI),[238] in which configurations are built out of (single-configuration) SCF orbitals, and multiconfiguration self-consistent-field (MCSCF)[239] methods, in which the orbitals are reoptimized in a multiconfigurational context.

The most systematic MCSCF approach is one in which the configurations included in the MCSCF are all those which can be formed by distributing the valence electrons among a set of 'active" orbitals, subject to spin and symmetry considerations. Such an MCSCF is called a complete active space self-consistent field (CASSCF).[240,241] If one includes all occupied valence orbitals and their antibonding counterparts as active orbitals, this is referred to as a fully optimized reaction space (FORS)[242,243] calculation. A simplier version of the FORS model is to include in the active space only those orbitals which are directly involved in the reaction to be described. One might, for example, neglect the methyl CH electrons in the reaction $CH_3 + H_2 \rightarrow CH_4 + H$. In general the orbitals included in the active space must be carefully chosen to provide a consistent description of the system at all geometries of interest.

A widely employed level of CI is to include all doubly (CID) or all singly and doubly (CISD) excited configurations relative to an SCF reference configuration or to a reference set of configurations. A single-reference CI is frequently corrected for the neglect of unlinked quadruple excitations using a formula due to Davidson.[244] This will be referred to below as the Davidson quadruples (+Q) correction, leading to CID+Q or CISD+Q. Because a single configuration often does not provide an equally valid reference over the whole reaction path, a large CI calculation is often preceded by a smaller MCSCF calculation. A multireference CI may then be performed, including some subset of excitations relative to the reference configurations included in the MCSCF. A particularly accurate wave function is obtained, for example, if one includes all single and double excitations relative to the FORS reference set. This is sometimes referred to as a second-order CI (SOCI).[245] Other workers use the SOCI description for a CI allowing all possible occupations of up to two holes in the valence space and up to two electrons in the virtual space. A very effective smaller CI, referred to as (PolCI),[246] restricts the double excitations to those for which only one electron leaves the active space. The PolCI approach is usually used with a special case of the MCSCF wave function, namely the generalized-valence-bond (GVB)[247,248] approximation.

Perturbation theory methods have largely been developed by the groups of Bartlett[249] and Pople.[250] The most popular approach is the *n*th-order Moller–Plesset method (MP*n*), where *n* typically is 2, 3, or 4.[250] The perturbation theory results may be extrapolated to higher orders by the use of Padé approximants.[251] Both CI and perturbation-theory calculations may be extrapolated to the limit of a complete basis set and infinite-order correlation by scaling the correlation energy.[252,253]

Coupled cluster (CC) methods[108,254-258] provide a third alternative (to CI and MBPT). Although they have not been applied to calculate full polyatomic potential surfaces as yet, such applications should be expected. Coupled cluster methods, like MBPT and unlike CI, are size extensive.

It is convenient to use the notation X/Y to describe the level of electronic structure where X denotes the form of the many-electron wave function and Y denotes the one-electron basis. A common procedure is to determine the energetics of a reaction at a more accurate computational level, say A/B, than that used to determine the structures at the stationary points or along the reaction path, say C/D. This will be indicated by the notation A/B//C/D, which has become a standard description.

A. Three-Atom Systems

As a test of their IRC approach, Ishida, Morokuma, and Komornicki[202] investigated the isomerization of HCN to HNC, at the SCF/STO-3G level. While these

authors did not calculate rate constants or vibrational frequencies along the reaction path, a more extensive calculation by Gray et al.[259] did address these issues. The latter authors determined the MEP for the isomerization at the SCF/DZP level. A rather large step size along the reaction coordinate, 0.1 $u^{1/2}$Å, was used, followed by a manual smoothing of the resulting oscillations. The SCF frequencies along the reaction path were scaled by a factor chosen to reproduce CI frequencies calculated at the saddle point, in order to better represent $V_a^G(s)$. The adiabatic potential function resulting from CI energetics and scaled SCF frequencies was then fit to an Eckart function. The vibrational coupling matrix elements are strongest between the reaction coordinate and the H–CN stretch. From calculations based on the reaction-path Hamiltonian, the authors concluded that tunneling yields observable rates at energies as much as 8 kcal/mol below the classical threshold. Over the physically significant energy region, the nonseparable vibrational coupling elements did not appear to influence the tunneling probability to a large extent. This reaction and the related isomerization of methyl nitrile have also been studied with perturbation theory by Redmon, Purvis, and Bartlett,[260,261] and Saxe et al.[262] also investigated the methyl nitrile system, but no reaction paths were determined by these authors.

B. Four-Atom Systems

Because of its importance as a prototypical photochemical, as well as thermal, system, formaldehyde has been the subject of a large number of electronic structure and dynamics calculations. A global PES for this system is discussed in section II.B. Jaffe, Hayes, and Morokuma[263] carried out calculations on this system at the CI/4-31G level for more than 200 geometries as a function of the distance between the CO and H_2 fragments for the ground state and the first excited singlet and triplet states; however, neither an MEP nor a force constant matrix was calculated. Jaffe and Morokuma[264] subsequently located the ground-state saddle point for the H_2CO decomposition with a small MCSCF using the same basis set. Based on a previous calculation by Goddard and Schaefer,[265] Miller[266] used $V_a^G(s)$ to investigate the tunneling corrections for the decomposition reaction and demonstrated that tunneling has a dramatic effect at energies well below the classical barrier.

The first MEP calculations for the formaldehyde decomposition reaction were performed by Fukui and co-workers. A MINDO/3 IRC for this reaction[267] was followed by an SCF/4-31G study.[268] In the latter study it was found that the variation in the vibrational frequencies and the coupling between the generalized normal modes along the minimum energy path are both significant. By following the character of the generalized normal modes from the reactant to the transition state, the authors suggest that the 1377 cm^{-1} antisymmetric deformation mode of H_2CO, which is strongly coupled to the CH symmetric stretch, initially promotes the reaction. The vibrational frequencies along the decomposition pathway were compared graphically to those for the isomerization reaction leading to HCOH. Both the variation in the generalized normal-mode frequencies and the intermode couplings were found to be much smaller for the isomerization, but once again it appears that the reaction is originally promoted by the 1377 cm^{-1} antisymmetric deformation.

The most accurate set of calculations on the formaldehyde surface are those by Gray et al.,[269] who employed both DZ and DZP basis sets and a CISD wavefunction. The authors investigated 20 evenly spaced points along the MEP between $s = \pm 0.21$ $u^{1/2}$Å. These points were fit to an Eckart potential[270] chosen to have the same curvature and barrier height as the ab initio calculations. The force constants, excluding the out-of-plane bend, were calculated at the two end points and combined with those at the saddle point to evaluate the vibrational coupling matrix elements. In contrast with the conclusions of Yamashita, Yamabe, and Fukui,[268] these authors concluded that the intermode couplings are small. The calculated rate constants were found to be sensitive to the level of ab initio calculation, but not to small errors in the vibrational frequencies. Semiclassical tunneling calculations indicate that, as one would expect, tunneling increases the calculated rate constants at low energy. Incorporation of intermode coupling has the opposite effect. Although no MEP or rate constant calculations were carried out, the most accurate values for the classical barrier heights for both the decomposition and isomerization reactions have recently been calculated by Frisch, Binkley, and Schaefer,[271] by using fourth-order perturbation theory and extensive basis sets. The two barriers are found to be greater than 80 kcal/mol and within 1 kcal/mol of each other.

Harding and Wagner[272] calculated MEP's for the reactions $H + HCO \rightarrow H_2 + CO$ and H_2CO at the CASSCF/DZP level. Both reactions appear to proceed without a barrier so the MEP must be followed in "from infinity", as done previously[166] for atom–diatom collisions. These calculations were used then as a starting point for full VTST calculations, which include the effect of orbital orientation constraints as entropic factors.[272,273]

Two molecules closely related to formaldehyde have also been investigated. Morokuma, Kato, and Hirao[218,274] have probed the decomposition and isomerization reactions of HFCO at the CISD+Q/6-31G(d,p)//SCF/4-31G level of computation. In contrast with formaldehyde, the decomposition is predicted to have a 25 kcal/mol lower barrier than the isomerization. Analysis of the decomposition IRC suggests that the fluorine moves away first, followed by a large motion of the hydrogen, but neither force constants nor rate constants were evaluated.

Tachibana and co-workers[275] have studied the analogous reactions for H_2CS at the CID+Q/6-31G(d,p)//SCF/6-31G(d,p) level. As noted above for formaldehyde, the two calculated barriers are large and only separated by a few kcal/mol. For the decomposition reaction, the out-of-plane frequency becomes imaginary along the MEP, leading to a valley-ridge inflection point that reduces the symmetry of the reaction path from C_s to C_1. This increases the amplitude of vibrational fluctuations about the symmetry-restricted MEP and broadens the dissociation channel. Unimolecular rate constants were obtained using RRKM theory[276] including tunneling corrections. Again tunneling was found to be substantial at energies below the classical

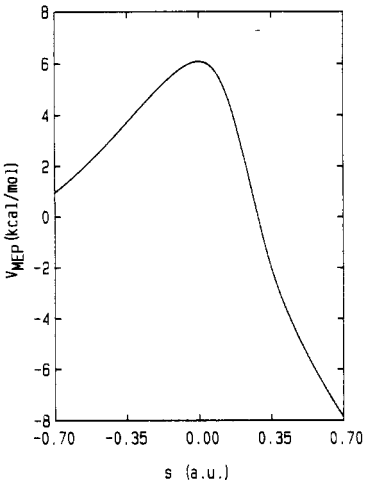

Figure 1. Classical potential energy along the reaction coordinate for OH + H_2 → H_2O + H. The variables plotted and zero of energy are defined below equation 2.

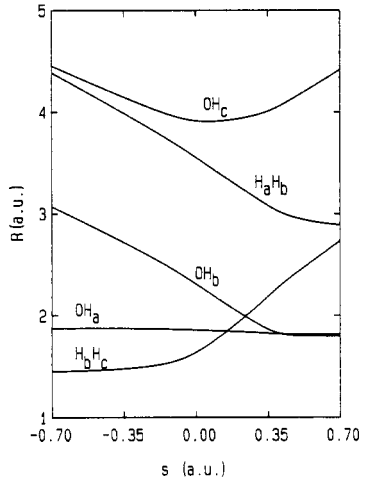

Figure 2. Internuclear distances along the reaction path for the reaction H_aO + H_bH_c → H_aOH_b + H_c as a function of the reaction coordinate.

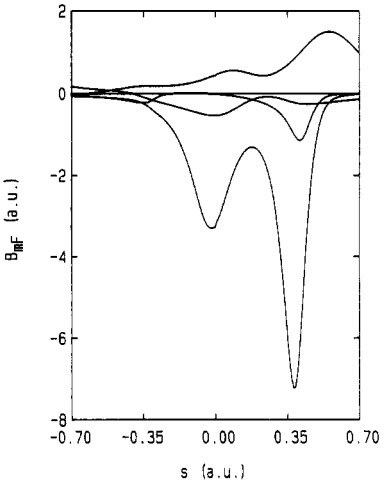

Figure 3. Components of the reaction-path curvature (see equation 3) along the reaction coordinate. Note that each component is arbitrary within an overall sign. The signs have been chosen for clarity of display.

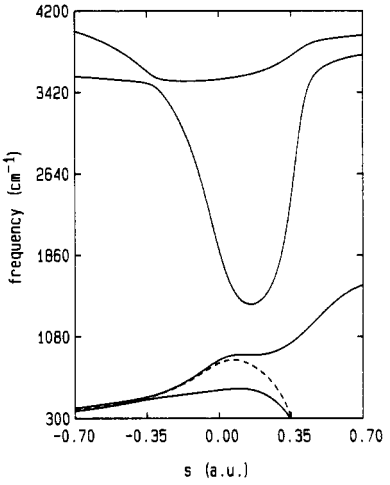

Figure 4. Generalized normal mode frequencies for vibrational modes orthogonal to the reaction path as a function of the reaction coordinate.

barrier height. In very recent work Tachibana et al.[277] have studied the decomposition H_2SiO → H_2 + SiO. They found that as the molecule dissociates the force constant for the out-of-plane bend becomes negative, and they discussed the consequences of this for the barrier shape for dissociation by tunneling.

Two calculations have been carried out by Schaefer, Miller, and co-workers[278,279] on the rearrangement of vinylidene (H_2C=C) to acetylene. Experimentally, the isomerization appears to occur rapidly, with a vinylidene lifetime estimated to be on the order of picoseconds. Equilibrium and transition-state structures were determined at the CISD/DZP level with analytical CI gradients. Single points calculated with a larger basis set, a Davidson correction, and an estimate for remaining errors resulted in a predicted barrier of 4 kcal/mol.[278] This is somewhat higher than expected based on the experimental results; however, the calculations suggest that tunneling causes a large increase in the calculated rate. This results in a predicted vinylidene lifetime in good agreement with experiment. In a more sophisticated calculation,[279] the energy derivatives were obtained at the CISD/TZP level. Using a quadratic interpolation scheme, the authors estimated the matrix elements coupling the reaction path to the remaining $3N - 7$ orthogonal vibrational modes and then constructed a reaction-path Hamiltonian. For a 4 kcal/mol barrier the vinylidene lifetime was found to be significantly affected by these coupling terms, in agreement with the results of the earlier paper. Tunneling was again found to be important, and one quantum of vibrational excitation in the vinylidene scissor mode is predicted to reduce the lifetime by a factor of 2.

Isaacson and Truhlar[93,95] have investigated the reactions OH(n_{OH} = 0,1) + H_2(n_{HH} = 0,1) → H_2O + H, where n_{OH} and n_{HH} are vibrational quantum numbers, using a reaction-path potential based on the global potential energy surface[90-92] discussed in section II.B. In the notation used here this is an analytic fit of a PolCI/TZP potential energy surface. Figures 1–4 present some reaction-path properties computed from this global surface, with each figure having the same reaction-coordinate scale to aid in the comparisons. Figure 1 shows the reaction-path potential as a function of distance along the MEP. The change in the internuclear distances along the reaction path are shown in Figure 2. In this figure the hydrogen atoms are labeled such that H_aO + H_bH_c → H_aOH_b + H_c. The reaction-path curvature components are given in Figure 3. The

final figure of this series, Figure 4, shows the generalized normal-mode frequencies for vibrational modes orthogonal to the reaction path. Figure 1 shows that the reaction is exoergic so the bulk of the barrier occurs to the left of $s = 0$. Figure 2 shows that one bond distance, OH_a, is a spectator. The frequency for this mode is nearly constant at about 3500 cm^{-1}, except for two avoided crossings. The other nonzero frequency of the reactants is associated with the breaking H_bH_c bond, and as the system progresses along the reaction path, it becomes associated with the forming OH_b bond. The H_aH_b next-nearest-neighbor distance decreases monotonically, and the OH_c next-nearest-neighbor distance shows a local minimum. The dynamics calculations using this data were based on variational-transition-state theory, with tunneling included, using the small-curvature approximation. Neglect of reaction path curvature would result in much smaller quantal effects for the ground-state reaction. Anharmonicity was incorporated with Morse and quadratic–quartic models, and was also found to be important. The rate of decrease of the OH_bH_c stretching frequency was found to be very important in determining the bottleneck location and the magnitude of the enhancement for vibrational excitation of H_2. Thus, conventional transition-state theory is not adequate for this excited-state reaction, but variational transition-state theory provides reasonable predictions.

Other examples where the MEP for a polyatomic system has been found by following the negative of the gradient of an analytic surface with a numerical integrator include $H + CH_3 \rightarrow CH_4$[280] and $Li^+ + H_2O \rightarrow Li(H_2O)^+$.[281]

Russegger has studied the photoisomerization of imines using methyleneimine as an example.[282-284] In his model, Russeger separates the coordinates into "relevant" and "non-relevant" subsets. For methyleneimine, the former are chosen to be the inversion and rotation motions. The first and second derivatives for the remaining $3N - 8$ coordinates were calculated as a function of these two for both the S_0 and T_1 states, using an SCF/DZ wave function, and strong coupling between the inversion and CH and NH stretching motions was found in both states, whereas the coupling between the rotation and stretches is weak. The two "relevant" modes are strongly coupled.

Swanson et al.[285] have provided an interesting semiempirical study of the dissociative reactions of BF_3 and SO_3. This study illustrates how information about the coupling of internal coordinates in the vicinity of a potential minimum, as determined by vibrational spectroscopy, can be extrapolated to give information about the dissociation pathway, especially if augmented by electronic structure calculations. This approach had been applied earlier to the dissociation of several triatomics by Machida and Overend.[286]

C. Five-Atom Systems

Besides the global surface discussed in section II.C., the potential energy surface for the decomposition of methane to methyl + H has been the subject of two recent calculations, one at the MP4/6-31G(d,p)[287] level and the other at the FORS-SOCI/6-311++G(df,p)[288] level. While neither calculation involved the evaluation of force constants along the reaction path, they are important to mention here because, while both calculations predict the net reaction energetics with reasonable accuracy, the potential at intermediate CH bond lengths does not appear to be well represented by the MP4 surface.[288,289] Padé extrapolation of the perturbation theory results[287,290] gave significant improvement, and it also appears that projection of spin-contaminated components of the UHF reference state leads to significant improvement in perturbation theory calculations of potential curves along bond dissociation coordinates.[291] The bond distance and dissociation energy of CH_4, but not other points on the surface, had also been calculated in an even larger multireference CI calculation, involving 613 941 configurations.[292]

Another dissociation reaction of methane is the molecular elimination of H_2 to form closed-shell methylene. The reverse of this reaction is a prototype for carbene insertion reactions. Wang and Karplus[293] generated a minimum energy path with CNDO and then investigated classical trajectories for this system by integrating the equations of motion. This process was also investigated by Bauschlicher et al.[294] These authors calculated more than 600 points on the surface at the CI/DZ level. These calculations were the first to establish that the non-least-motion path is monotonically downhill, even though the least-motion path is symmetry forbidden. Gordon and co-workers[295] have analyzed the analogous SiH_4 surface. (A global PES for the decomposition of SiH_4 is discussed in section II.C.) The IRC generated with a FORS/6-31G(d) wavefunction leads smoothly to silane at one end and $SiH_2 + H_2$ at the other. However, single points along this path with larger basis sets and either SOCI or fourth-order perturbation theory indicate the presence of a long-range minimum on the surface between the saddle point and the separated fragments. Refinements with MP2 and a TZP basis set verify the existence of the second minimum, and single points with MP4 and a very large basis set predict that the classical barrier, which in fact separates the second minimum from silane, is actually below the completely separated fragments. This finding agrees well with the most recent experimental estimates that the barrier is 1 kcal/mol or less. Minimum energy paths have also been calculated at a somewhat lower computational level (MP3/6-31G(d)//SCF/3-21G) for the insertions of CH_2 and SiH_2 into methane and silane.[296]

Two calculations have recently been carried out on the ground-state rearrangement of the methoxy radical to CH_2OH.[297,298] This surface has an interesting feature, since methoxy and the transition state both have C_s symmetry, whereas the isomerization product is C_1. This means that a second imaginary frequency must appear at some point on the (C_s-constrained) minimum energy path. Apparently, this occurs far enough along the MEP that reaction rate calculations are not seriously affected by it. In the first paper, Colwell[297] used FORS wave functions with both STO-3G and DZ basis sets. A gradient following algorithm was used to follow the MEP, with a step size of 0.1 $u^{1/2}a_0$. Although a smooth MEP was obtained, the use of such a large step size may mean that the MEP is not well converged. Tunneling, calculated assuming zero reaction-path curvature, is predicted to be important for the microcanonical rate constant down to 7000 cm^{-1} below the

classical threshold. The temperature-dependent rate constant increases by several orders of magnitude at low temperatures when tunneling is included. In the second paper,[298] reaction-path curvature effects were incorporated into the calculation using the RPH formalism. Here, the step size along the MEP was reduced to 0.05 $u^{1/2}a_0$ from the saddle point down to 8000 cm^{-1} below the saddle point. Below this, the original 0.1 $u^{1/2}a_0$ step size was retained. In addition to the force constants, dipole moments, polarizabilities, dipole-moment derivatives, and vibrational-coupling-matrix elements were calculated at each point on the reaction path. With tunneling included, but assuming zero curvature, the microcanonical rate constant was calculated to increase slowly as the energy is increased from 8000 cm^{-1} below the barrier. Incorporation of curvature reduces the calculated rate constant at very low energies, but increases the rate as the barrier is approached. Temperature-dependent rate constants calculated with tunneling included are much greater than those in which tunneling is neglected. Curvature has a similar effect as it does for the microcanonical rate constant.

Yamashita and Yamabe[299] used SCF/4-31G wave functions to investigate the IRC's for the decomposition of formic acid to two sets of products: $H_2 + CO_2$ via a 4-center transition state and $H_2O + CO$ via a 3-center transition state. For the 3-center transition state, coupling between the IRC and perpendicular vibrational modes is small, as is the curvature of the reaction path. On the other hand, the curvature of the minimum-energy path for the elimination of CO_2 is large, as a consequence of coupling with the OH and CH stretching modes of HCOOH. This suggests that energy transfer into these modes will be significant.

D. Six-Atom Systems

The most frequently studied six-atom surface is that for the reaction $CH_3 + H_2 \rightarrow CH_4 + H$. Semiempirical global PESs for this reaction are discussed in section II.A. The first ab initio investigation of this surface was the calculation by Morokuma and Davis.[300] These authors used both minimal and DZ Slater basis sets within the ROHF formalism. Geometries at the SCF level were followed by single-point PolCI calculations. Both the abstraction and substitution reactions were investigated, and a number of points were calculated for each reaction surface. Fukui and co-workers[301,302] used the STO-3G basis set and a small CI to demonstrate the decomposition of the gradient along the IRC into physically meaningful components. These authors also used the Hellmann–Feynmann theorem to partition the gradient into polarization, exchange, and delocalization contributions. More recently, Yamashita and Yamabe[299] generated the IRC and vibrational frequencies along the IRC for the abstraction reaction at the SCF/4-31G level. The authors concluded that the IRC consists primarily of relative translational motion of methyl and H_2 in the reactant region and relative translational motion of H and methane in the product region. The curvature of the IRC has two sharp peaks, one before and one after the saddle point, due to strong coupling with the H–H and C–H modes, respectively. (The double peaked character of the reaction-path curvature has been observed for many atom–diatom reactions in our VTST and semiclassical tunneling calculations.[303]) The most extensive calculations on the forward and reverse barriers for $CH_3 + H_2 \rightarrow CH_4 + H$ are the PolCI/DZP calculations of Walch[124b] and the MP4/6-311++G(3df,2pd)//SCF/6-31G(d) calculations of Gordon and Truhlar.[243] The PolCI forward and reverse barriers are too high by about 1–2 kcal/mol, respectively, while the MP4 results are too high by about 4–5 kcal/mol. There is little difference between the SCF/6-31G(d) saddle-point geometry and a more accurate MP2/6-311G(d,p) one.[253]

The related $H^- + CH_4$ nucleophilic substitution reaction was used by Ishida, Morokuma, and Komornicki[202] to demonstrate their procedure for determining the IRC. The same reaction was used by Joshi and Morokuma[304] to demonstrate their scheme for decomposing the force along the IRC into several components. Both calculations were at the SCF/STO-3G level.

Kato and Morokuma[218–220,305] analyzed several elimination and isomerization reactions of vinyl fluoride in its (closed shell) ground state and first excited triplet state at the SCF/4-31G level. (The SCF calculations were performed at the RHF level for closed shells and at the UHF level for open shells.) They also performed two-configuration MCSCF calculations for the internal rotation in the singlet case. Minimum energy paths were determined for the 3- and 4-center eliminations of HF on the singlet surface, and unimolecular rates were calculated with RRKM theory, including tunneling corrections. Tunneling has a larger effect on the four-center elimination, for which it can increase the rate by a factor of 3 near threshold. Since the two reactions are found to have similar classical barriers, the four-center elimination is predicted to be faster in the low energy region, while this is reversed at higher energies. The distribution of the excess energy among the vibrational modes was estimated in the weak and strong (statistical) coupling limits.

Yamashita, Yamabe, and Fukui[306] determined the minimum energy path for the four-center elimination of HF from CH_2F–OH, at the SCF/4-31G level. The energetics of the reaction were obtained at the CISD+Q level. At early stages of the reaction the IRC is dominated by the CF stretching and OCF bending motions. As the transition state is approached, the COH bending contribution becomes important. As the reaction proceeds to products, the IRC looks increasingly like the relative translational motion of the fragments. The OH stretch of the parent becomes the HF stretch in the product. The lifetime of the reactant, which is assumed to have been formed by an insertion, $O(^1D) + CH_3F \rightarrow CH_2F$–OH, and to decay by HF elimination, was taken to be the reciprocal of the RRKM rate constant and was calculated as a function of the total energy E of the system. Near the threshold energy of 50 kcal/mol, the lifetime is 10^{-5} s, but for E = 140 kcal/mol (estimated to be the energy available experimentally) the lifetime is $<10^{-12}$ s, roughly the period of a vibration. Thus, randomization of energy is more likely near threshold. In the absence of randomization, the OCF bend and OH stretch lead to rotational and vibrational excitation of HF, respectively. For longer lifetimes, coupling in the exit valley will play an important role.

E. Systems with Seven–Ten Atoms

Although the minimum energy path was not obtained directly, Hase et al.[127] used UHF/STO-3G calculations to generate about 2000 points on the H + C_2H_4 surface. The attacking H*--C distance was chosen to be the distinguished coordinate, with other selected internal coordinates being optimized as a function of R(H*--C). The harmonic force constants were calculated as a function of R(H*--C) and R(C--C). Global fits to the C_2H_5 surface are discussed in section II.E. In a related paper, Kato and Morokuma[307] used UHF/4-31G wave functions to investigate the decomposition of H_2CCH_2F to vinyl fluoride + atomic hydrogen. As for the previous work, R(C--H*) was chosen to be the distinguished coordinate, with all other parameters being optimized as a function of this bond length. Extensive mixing is found to take place among all of the vibrational modes on going from the reactant to the loose transition state. Thus, nearly all of the modes can participate in energy transfer during the dissociation process. At the transition state, the reaction coordinate is mainly composed of the relative translational motion of the fragments. Three of the CH stretching frequencies have about the same values at the transition state as in the product, and these are regarded as adiabatic. On the other hand, the CC stretch is strongly coupled with the CH_2 bend and the CH planar deformation, while the out-of-plane bend couples with the CH_2 rock. Redistribution of kinetic energy among these coupled modes is most likely. Tunneling was estimated using a transmission coefficient for an inverted parabolic potential barrier in one dimension. Tunneling is predicted to have a large effect on the rate and the reactant lifetime at low energies. More recent calculations have demonstrated[308,309] that an accurate treatment of radical reactions with ethylene requires the use of either MCSCF or spin-projected UHF-based wave functions.

The molecule formamidine (methanimidamide) has generated some interest because its degenerate rearrangement, $HN{=}CHNH_2 \rightleftarrows H_2NCH{=}NH$, is a prototype for hydrogen transfer between bases in biosystems. Yamashita and co-workers[310] studied the IRC for this proton transfer at the SCF/4-31G level, and they predicted a large (59 kcal/mol) barrier. In a later paper, they calculated that the addition of a water molecule to the system[311] reduces the barrier substantially, since the proton transfer is aided by two hydrogen bonds between the two molecules and a double proton exchange. They also calculated the semiclassical tunneling probability for H and D transfer as a function of the energy available to the system. This leads to a significant isotope effect which was attributed to the difference in the effective masses for hydrogenic motion along the MEP. In particular, in non-mass-scaled coordinates, the effective mass for the protonated species is approximately constant along the IRC, whereas there is considerable variation for the deuterated species. This conclusion, however, was obtained without including the effect of reaction-path curvature, which may be significant. More recently, two of the authors have reinvestigated the proton transfer, with and without the water present, at a number of computational levels.[312] At the highest level, MP4/6-311G(d,p)//SCF/6-31G(d), the barriers with and without the water are 25 and 48 kcal/mol, respectively. The formamidine IRC has been calculated at the SCF/STO-3G level with a very small step size, in preparation for semiclassical tunneling calculations to study the effect of including reaction-path curvature effects.

Kato and Morokuma[187] have developed an analysis of the IRC which is based on classifying of the vibrational motions into statistical and dynamical modes. The former are essentially observer modes with small reaction-path curvature components along the entire IRC, while the latter participate directly and strongly in the reaction dynamics. This allows the energetics of the reaction to be partitioned into a statistically determined factor (depending only on the normal frequencies at the transition state and product) and dynamically determined factors (depending on the detailed nature of the potential energy surface). The method was demonstrated[187,218–220] for the decomposition of ethyl fluoride into ethylene + HF. Geometries, force constants, and the IRC were determined at the SCF/4-31G level, while the energetics were obtained at the CISD+Q/4-31G level. Near the transition state, the IRC is mainly composed of the HF stretching motion. As the reaction proceeds, the relative translation of the fragments becomes more important. Interchange of these two components in the intermediate region of the IRC results in large reaction-path curvature in this region. Most of the excess energy from the transition state is predicted to end up in the vibrational motion of the fragments. The HF stretch is a dynamical mode and interacts strongly with the IRC. Four other vibrations, including the CC stretch and CH_2 wag, couple weakly with the IRC. Energy transfer into these modes becomes important late in the reaction. The remaining 12 modes are classified as statistical.

Fukui and co-workers[313] analyzed the hydrogen transfer reaction in malonaldehyde using the semi-empirical CNDO/2 method. A reaction-path Hamiltonian was obtained within the zero-curvature vibrationally adiabatic approximation, using generalized normal coordinates calculated at several points along the IRC. The potential along the reaction coordinate was fit to the sum of an eighth-order polynomial and a gaussian function, and a vibrational basis set consisting of 20 harmonic functions was used to obtain the vibrational eigenfunctions and eigenvalues. As the temperature is increased from 0 to 500 K, the equilibrium density profile along the reaction coordinate is transformed from a double-humped function to one with a single central maximum. The proton transfer rate was calculated quantum mechanically from the time evolution operator of the double-well eigenstates. This reaction was also studied by Miller, Schaefer, and co-workers.[314–316] In the first study[314] they calculated only the stationary points using a double-zeta basis set with p functions on the migrating hydrogen, with the barrier[315] height estimated using CISD+Q method. In a later paper they used minimum basis set SCF calculations scaled to an MP4/6-31G(d,p)//MP2/6-31G(d,p) barrier height[316] to obtain a two dimensional fourth-order-polynomial representation of the PES, which was used, in conjunction with an adiabatic treatment of the other modes, to semiclassically estimate the tunneling splitting in the ground vibrational state.

Ohmine and Morokuma[317,318] have investigated the photoisomerization of polyenes. The IRC's for the ground and lowest triplet states of butadiene and longer

polyenes and the protonated Schiff base of butadiene were analyzed using the UHF/STO-3G, UHF/4-31G, and MINDO/3 methods. Classical trajectories were determined by integrating the classical equations of motion. Decay of the CC torsional motion, by transferring its energy into other internal modes, was found to be very slow. Many torsional oscillations occur before the system decays to its lowest torsional state. If enough energy is added to the system one torsion can couple with and transfer energy to another, inducing double torsional motion before dissipation into other modes.

Yamabe et al.[319] performed IRC analyses for the unimolecular dissociations of C_2H_5OH to yield C_2H_4 or CH_3CHO. The IRC was calculated at the RHF/4-31G level, and reactants and products were investigated at the CI/4-31G//RHF/4-31G level. The IRC analysis was used to discuss the coupling of vibrational modes to the reaction coordinate.

IV. Concluding Remarks

Theoretical polyatomic reaction dynamics is at a significant stage of development. The tools of electronic structure theory and dynamics methods have both matured considerably in the last few years, and increased computing power is becoming available to exploit these tools. The techniques of fitting potential surfaces are not as well developed though, and each new fit still appears to require very much specialized attention. Nevertheless, by a combination of both global-surface fits and reaction-path potentials, we expect dramatic progress to result from the combination of electronic structure calculations and dynamics techniques in the next few years.

V. Acknowledgments

The authors are grateful to Dr. Franklin B. Brown for his assistance in the early stages of this review project. This work was supported in part by the National Science Foundation under grant number CHE83-17944 and by the University of Minnesota Supercomputer Institute.

VI. References

(1) *Atom-Molecule Collision Theory*; Bernstein, R. B., Ed.; Plenum: New York, 1979.
(2) *Potential Energy Surfaces and Dynamics Calculations*; Truhlar, D. G., Ed.; Plenum: New York, 1981.
(3) Bernstein, R. B. *Chemical Dynamics via Molecular Beam and Laser Techniques*; Oxford University: New York, 1982.
(4) *Energy Storage and Redistribution in Molecules*; Hinze, J., Ed.; Plenum: New York, 1983.
(5) Pritchard, H. O. *The Quantum Theory of Unimolecular Reactions*; Oxford University: Cambridge, 1984.
(6) Murrell, J. N.; Carter, S.; Farantos, S. C.; Huxley, P.; Varandas, A. J. C. *Molecular Potential Energy Surfaces*; Wiley: New York, 1984.
(7) Sathyamurthy, N. *Comput. Phys. Rep.* **1985**, *3*, 1.
(8) Dunning, T. H., Jr.; Harding, L. B. In *Theory of Chemical Reaction Dynamics*, Baer, M., Ed.; CRC: Boca Raton, FL, 1985; Vol. 1, p 1.
(9) Kuntz, P. J., ref 8, Vol. 1, p 71.
(10) Herzberg, G. *Molecular Spectra and Molecular Structure. III. Electronic Spectra and Electronic Structure of Polyatomic Molecules*; Van Nostrand Reinhold: New York, 1966; p 9.
(11) Fischer, G. *Vibronic Coupling*; Academic: London, 1984; p 33.
(12) Polanyi, J. C.; Schreiber, J. L. *Chem. Phys. Lett.* **1974**, *29*, 319.
(13) (a) Bender, C. F.; O'Neil, S. V.; Pearson, P. K.; Schaefer, H. F., III. *Science (Washington, D.C.)* **1973**, *176*, 1412. (b) Steckler, R.; Schwenke, D. W.; Brown, F. B.; Truhlar, D. G. *Chem. Phys. Lett.* **1985**, *121*, 475.
(14) Liu, B. *J. Chem. Phys.* **1973**, *58*, 1925.
(15) Siegbahn, P.; Liu, B. *J. Chem. Phys.* **1978**, *68*, 2457.
(16) Truhlar, D. G.; Horowitz, C. J. *J. Chem. Phys.* **1978**, *68*, 2466; **1979**, *71*, 1514(E).
(17) London, F. *Z. Elektrochem.* **1929**, *35*, 552.
(18) Varandas, A. J. C.; Brown, F. B.; Mead, C. A.; Truhlar, D. G.; Blais, N. C., manuscript in preparation.
(19) Howard, B. E.; McLean, A. D.; Lester, W. A. *J. Chem. Phys.* **1979**, *71*, 2412.
(20) Schinke, R.; Lester, W. A. *J. Chem. Phys.* **1979**, *70*, 4893.
(21) Walch, S. P.; Dunning, T. H.; Raffenetti, R. C.; Bobrowicz, F. W. *J. Chem. Phys.* **1980**, *72*, 406.
(22) Schatz, G. C.; Wagner, A. F.; Walch, S. P.; Bowman, J. M. *J. Chem. Phys.* **1981**, *74*, 4984.
(23) Walch, S. P.; Wagner, A. F.; Dunning, T. H., Jr.; Schatz, G. C. *J. Chem. Phys.* **1980**, *72*, 2894.
(24) Dunning, T. H., Jr.; Walch, S. P.; Wagner, A. F. In *Potential Energy Surfaces and Dynamics Calculations*; Truhlar, D. G., Ed.; Plenum: New York, 1981; p 329.
(25) Garrett, B. C.; Truhlar, D. G. *Int. J. Quant. Chem.* **1986**, *29*, 1463.
(26) Garrett, B. C.; Truhlar, D. G.; Wagner, A. F.; Dunning, T. H. *J. Chem. Phys.* **1983**, *78*, 4400.
(27) Sathyamurthy, N.; Raff, L. M. *J. Chem. Phys.* **1975**, *63*, 464.
(28) Sathyamurthy, N.; Rangarajan, R.; Raff, L. M. *J. Chem. Phys.* **1976**, *64*, 4606.
(29) Brown, P. J.; Hayes, E. F. *J. Chem. Phys.* **1971**, *55*, 922.
(30) Chen, M. M. L.; Schaefer, H. F., III. *J. Chem. Phys.* **1980**, *72*, 4376.
(31) Carter, S.; Murrell, J. N. *Mol. Phys.* **1980**, *41*, 567.
(32) Alvariño, J. M.; Gervasi, O.; Laganâ, A. *Chem. Phys. Lett.* **1982**, *87*, 254.
(33) Alvariño, J. M.; Hernandez, M. L.; Garcia, E.; Laganâ, A. *J. Chem. Phys.* **1986**, *84*, 3059.
(34) Schor, H.; Chapman, S.; Green, S.; Zare, R. N. *J. Chem. Phys.* **1978**, *69*, 3790.
(35) (a) Chapman, S.; Dupuis, M.; Green, S. *Chem. Phys.* **1983**, *78*, 93. (b) Paniagua, M.; Sauz, J. C.; Alvariño, J. M.; Laganâ, A. *Chem. Phys. Lett.* **1986**, *126*, 330.
(36) Bowman, J. M.; Lee, K. T.; Romanowski, H.; Harding, L. B. In *Resonances in Electron–Molecule Scattering, van der Waals Complexes, and Reactive Chemical Dynamics*; Truhlar, D. G., Ed.; *ACS* Symposium Series 263; American Chemical Society, Washington, DC, 1984; p 43.
(37) Simons, G.; Parr, R. G.; Finlan, J. M. *J. Chem. Phys.* **1973**, *59*, 3229.
(38) Bowman, J. M.; Bittman, J. S.; Harding, L. B. *J. Chem. Phys.* **1986**, *85*, 911.
(39) Stroud, C.; Sathyamurthy, N.; Rangarajan, R.; Raff, L. M. *Chem. Phys. Lett.* **1977**, *48*, 350.
(40) Sathyamurthy, N.; Duff, J. W.; Stroud, C.; Raff, L. M. *J. Chem. Phys.* **1977**, *67*, 3563.
(41) Wagner, A. F.; Schatz, G. C.; Bowman, J. M. *J. Chem. Phys.* **1981**, *74*, 4960.
(42) Lee, K. T.; Bowman, J. M.; Wagner, A. F.; Schatz, G. C. *J. Chem. Phys.* **1982**, *76*, 3563.
(43) Lee, K. T.; Bowman, J. M.; Wagner, A. F.; Schatz, G. C. *J. Chem. Phys.* **1982**, *76*, 3583.
(44) Brown, F. B.; Steckler, R.; Schwenke, D. W.; Truhlar, D. G.; Garrett, B. C. *J. Chem. Phys.* **1985**, *82*, 188.
(45) Connor, J. N. L.; Jakubetz, W.; Manz, J. *Mol. Phys.* **1975**, *29*, 347.
(46) Muckerman, J. T. *Theor. Chem. (New York)* **1981**, *6A*, 1.
(47) Truhlar, D. G.; Garrett, B. C.; Blais, N. C. *J. Chem. Phys.* **1984**, *80*, 232.
(48) Steckler, R.; Truhlar, D. G.; Garrett, B. C. *J. Chem. Phys.* **1985**, *83*, 2870.
(49) Truhlar, D. G.; Wyatt, R. E. *Adv. Chem. Phys.* **1971**, *36*, 141.
(50) Westenberg, A. A.; de Haas, N. *J. Chem. Phys.* **1967**, *47*, 4241.
(51) Johnson, B. R.; Winter, N. W. *J. Chem. Phys.* **1977**, *66*, 4116.
(52) Bondi, D. K.; Connor, J. N. L.; Manz, J.; Romelt, J. *Mol. Phys.* **1983**, *50*, 467.
(53) Balint-Kurti, G. G.; Yardley, R. N. *Faraday Discuss. Chem. Soc.* **1977**, *62*, 77.
(54) Shapiro, M.; Zeiri, Y. *J. Chem. Phys.* **1979**, *70*, 5264.
(55) Kuntz, P. J.; Roach, A. C. *J. Chem. Phys.* **1981**, *74*, 3420.
(56) Roach, A. C.; Kuntz, P. J. *J. Chem. Phys.* **1981**, *74*, 3435.
(57) Ellison, F. O. *J. Am. Chem. Soc.* **1963**, *85*, 3540.
(58) Tully, J. C. In *Semi-Empirical Methods of Electronic Structure Calculation, Part A: Techniques*, Segal, G. A., Ed.; Plenum Press: New York, 1977; Chapter 6.
(59) Kuntz, P. J. In *Atom-Molecule Collision Theory*; Bernstein, R. B., Ed.; Plenum: New York, 1979; p 79.
(60) Last, I.; Baer, M. *J. Chem. Phys.* **1981**, *75*, 288.

(61) Baer, M. Last, I. *Potential Energy Surfaces and Dynamics Calculations*; Truhlar, D. G.; Plenum: New York, 1981; p 519.
(62) Viswanathan, R.; Thompson, D. L.; Raff, L. M. *J. Phys. Chem.* **1985**, *89*, 1428.
(63) Eaker, C. W.; Parr, C. A. *J. Chem. Phys.* **1976**, *64*, 1322.
(64) Sato, S. *Bull. Chem. Soc. Jpn.* **1955**, *28*, 450.
(65) Sato, S. *J. Chem. Phys.* **1955**, *23*, 592.
(66) Sato, S. *J. Chem. Phys.* **1955**, *23*, 2465.
(67) Parr, C. A.; Truhlar, D. G. *J. Phys. Chem.* **1971**, *75*, 1844.
(68) Kuntz, P. J.; Nemeth, E. M.; Polanyi, J. C.; Rosner, S. D.; Young, C. E. *J. Chem. Phys.* **1966**, *44*, 1168.
(69) Blais, N. C.; Truhlar, D. G. *J. Chem. Phys.* **1974**, *58*, 4186; **1976**, *65*, 3803(E).
(70) (a) Garrett, B. C.; Truhlar, D. G. *J. Chem. Phys.* **1980**, *72*, 3460. (b) Truhlar, D. G.; Isaacson, A. D.; Garrett, B. C. In *Theory of Chemical Reaction Dynamics*; Baer, M., Ed.; CRC: Boca Raton, FL, 1985; Vol. 4, p 65.
(71) Bunker, D. L.; Blais, N. C. *J. Chem. Phys.* **1964**, *41*, 2377.
(72) Bunker, D. L.; Parr, C. A. *J. Chem. Phys.* **1970**, *52*, 5700.
(73) Wall, F. T.; Porter, R. N. *J. Chem. Phys.* **1962**, *36*, 3256.
(74) Bowman, J. M.; Kuppermann, A. *Chem. Phys. Lett.* **1975**, *34*, 523.
(75) Johnston, H. S.; Parr, C. A. *J. Am. Chem. Soc.* **1963**, *85*, 2544.
(76) Johnson, H. S. *Adv. Chem. Phys.* **1960**, *3*, 131.
(77) Johnston, H. S.; Goldfinger, P. *J. Chem. Phys.* **1962**, *37*, 700.
(78) Sharp, T. E.; Johnston, H. S. *J. Chem. Phys.* **1962**, *37*, 1541.
(79) Carmichael, H.; Johnston, H. S. *J. Chem. Phys.* **1964**, *41*, 1975.
(80) Shefter, E. In *Transition States of Biochemical Processes*; Gandour, R. D.; Schowen, R. L., Eds.; Plenum: New York, 1978; p 353.
(81) Kafri, O.; Berry, M. J. *Faraday Discuss. Chem. Soc.* **1977**, *62*, 127.
(82) Garrett, B. C.; Truhlar, D. G. *J. Am. Chem. Soc.* **1979**, *101*, 4534.
(83) Garrett, B. C.; Truhlar, D. G. *J. Am. Chem. Soc.* **1979**, *101*, 5207.
(84) Garrett, B. C.; Truhlar, D. G.; Magnuson, A. W. *J. Chem. Phys.* **1982**, *76*, 2321.
(85) Schatz, G. C.; Wagner, A. F.; Walch, S. P.; Bowman, J. M. *J. Chem. Phys.* **1981**, *74*, 4984.
(86) Mayer, S. W. *J. Phys. Chem.* **1969**, *73*, 3941.
(87) Dmitrieva, I. K.; Zenevich, V. A.; Plindov, G. I. *Chem. Phys. Lett.* **1986**, *123*, 541.
(88) McLaughlin, D. R.; Thompson, D. L. *J. Chem. Phys.* **1973**, *59*, 4393.
(89) Benson, M. J.; McLaughlin, D. R. *J. Chem. Phys.* **1972**, *56*, 1322.
(90) Schatz, G. C.; Elgersma, H. *Chem. Phys. Lett.* **1980**, *73*, 21.
(91) Schatz, G. C.; Walch, S. P. *J. Chem. Phys.* **1980**, *72*, 776.
(92) Walch, S. P.; Dunning, T. H. *J. Chem. Phys.* **1980**, *72*, 1303.
(93) Isaacson, A. D.; Truhlar, D. G. *J. Chem. Phys.* **1982**, *76*, 1380.
(94) Isaacson, A. D.; Sund, M. T.; Rai, S. N.; Truhlar, D. G. *J. Chem. Phys.* **1985**, *82*, 1338.
(95) Truhlar, D. G.; Isaacson, A. D. *J. Chem. Phys.* **1982**, *77*, 3516.
(96) Rashed, O.; Brown, N. J. *J. Chem. Phys.* **1985**, *82*, 5506.
(97) Carter, S.; Mills, I. M.; Murrell, J. N. *Mol. Phys.* **1980**, *39*, 455.
(98) Carter, S.; Mills, I. M.; Murrell, J. N. *Mol. Phys.* **1980**, *41*, 191.
(99) Halonen, L.; Child, M. S.; Carter, S. *Mol. Phys.* **1982**, *47*, 1097.
(100) Swamy, K. N.; Hase, W. L. *Chem. Phys. Lett.* **1984**, *92*, 371.
(101) Dykstra, C. E.; Schaefer, H. F., III. *J. Am. Chem. Soc.* **1978**, *100*, 1378.
(102) Stine, J. R.; Muckerman, J. T. *J. Chem. Phys.* **1978**, *68*, 185.
(103) Bopp, P.; McLaughlin, D. R.; Wolfsberg, M. *Z. Naturforsch. A: Phys., Phys. Chem. Kosmophys.* **1982**, *37a*, 398.
(104) Maessen, B.; Bopp, P.; McLaughlin, D. R.; Wolfsberg, M. *Z. Naturforsch. A: Phys., Phys. Chem. Kosmophys.* **1984**, *38a*, 1005.
(105) Brown, F. B.; Tucker, S. C.; Truhlar, D. G. *J. Chem. Phys.* **1985**, *83*, 4451.
(106) Hancock, G. C.; Rejto, P.; Steckler, R.; Truhlar, D. G. *J. Chem. Phys.* **1986**, *85*, 4997.
(107) Barton, A. E.; Howard, B. J. *Faraday Discuss. Chem. Soc.* **1982**, *73*, 45.
(108) Michael, D. W.; Dykstra, C. E.; Lisy, J. M. *J. Chem. Phys.* **1984**, *81*, 5998.
(109) Raff, L. M. *J. Chem. Phys.* **1966**, *44*, 1202.
(110) Bunker, D. L.; Blais, N. C. *J. Chem. Phys.* **1962**, *37*, 2713.
(111) Karplus, M.; Raff, L. M. *J. Chem. Phys.* **1964**, *41*, 1267.
(112) Raff, L. M.; Karplus, M. *J. Chem. Phys.* **1966**, *44*, 1212.
(113) Chapman, S. *J. Chem. Phys.* **1981**, *74*, 1001.
(114) Viswanathan, R.; Raff, L. M. *J. Phys. Chem.* **1983**, *87*, 3251.
(115) Duchovic, R. J.; Hase, W. L.; Schlegel, H. B. *J. Phys. Chem.* **1983**, *88*, 1339.
(116) Viswanathan, R.; Thompson, D. L.; Raff, L. M. *J. Chem. Phys.* **1984**, *80*, 4230.
(117) McDonald, J. M.; Marcus, R. A. *J. Chem. Phys.* **1976**, *65*, 2180.
(118) Bunker, D. L.; Pattengill, M. D. *J. Chem. Phys.* **1970**, *53*, 3041.
(119) Valencich, T.; Bunker, D. L. *Chem. Phys. Lett.* **1973**, *20*, 50.
(120) Valencich, T.; Bunker, D. L. *J. Chem. Phys.* **1974**, *61*, 21.
(121) Chapman, S.; Bunker, D. L. *J. Chem. Phys.* **1975**, *62*, 2890.
(122) Raff, L. M. *J. Chem. Phys.* **1974**, *60*, 2220.
(123) Bunker, D. L.; Hase, W. L. *J. Chem. Phys.* **1973**, *59*, 4621. **1978**, *69*, 4711(E).
(124) (a) Bunker, D. L.; Goring-Simpson, E. A. *Faraday Discuss. Chem. Soc.* **1973**, *55*, 93. (b) Walch, S. P. *J. Chem. Phys.* **1980**, *72*, 4932.
(125) Schatz, G. C.; Walch, S. P.; Wagner, A. F. *J. Chem. Phys.* **1980**, *73*, 4536.
(126) Steckler, R.; Dykema, K.; Truhlar, D. G.; Valencich, T., manuscript in preparation.
(127) Hase, W. L.; Mrowka, G.; Brudzynski, R. J.; Sloane, C. S. *J. Chem. Phys.* **1978**, *69*, 3548.
(128) Grant, E. R.; Bunker, D. L. *J. Chem. Phys.* **1978**, *68*, 628.
(129) Sloane, C. S.; Hase, W. L. *Faraday Discuss. Chem. Soc.* **1977**, *62*, 210.
(130) Hase, W. L.; Bhalla, K. C. *J. Chem. Phys.* **1981**, *75*, 2807.
(131) Nagy, P. J.; Hase, W. L. *Chem. Phys. Lett.* **1978**, *54*, 73.
(132) Swamy, K. N.; Hase, W. L. *J. Chem. Phys.* **1986**, *84*, 361.
(133) Lu, D.; Hase, W. L.; Wolf, R. J. *J. Chem. Phys.*, in press.
(134) Sibert, E. L., III; Reinhardt, W. P.; Hynes, J. T. *J. Chem. Phys.* **1984**, *81*, 1115.
(135) Sibert, E. L., III; Hynes, J. T.; Reinhardt, W. P. *J. Chem. Phys.* **1984**, *81*, 1135.
(136) Steele, D. *J. Chem. Soc., Faraday Trans. 2* **1985**, 1077.
(137) Warshel, A.; Karplus, M. *J. Am. Chem. Soc.* **1972**, *94*, 5612.
(138) Burgi, H. B. *Angew. Chem., Int. Ed. Engl.* **1975**, *14*, 460.
(139) Veillard, A. In *Internal Rotation in Molecules*; Orville-Thomas, W. J., D.; Wiley: London, 1974; p 385.
(140) Viellard, A. In *Quantum Mechanics of Molecular Conformations*; Pullman, B., Ed.; Wiley: London, 1976; p 1.
(141) Momany, F. A.; McGuire, R. F.; Burgess, A. W.; Scheraga, H. A. *J. Phys. Chem.* **1975**, *79*, 2361.
(142) Warshel, A. In *Semiempirical Methods of Electronic Structure Calculation, Part A: Techniques*; Segal, G. A., Ed.; Plenum: New York, 1977; p 133.
(143) Burton, G. W.; Sims, L. B.; Wilson, J. C.; Fry, A. *J. Am. Chem. Soc.* **1977**, *99*, 3371.
(144) Allinger, N. L. *J. Am. Chem. Soc.* **1977**, *99*, 8127.
(145) Dunitz, J. D. *X-Ray Analysis and the Structure of Organic Molecules*; Cornell University: Ithaca, 1979.
(146) Burkert, U. B.; Allinger, N. L. *Molecular Mechanics*; American Chemical Society: Washington, DC, 1982.
(147) Sims, L. B.; Lewis, D. E. In *Isotopes in Organic Chemistry*; Buncel, E., Lee, C. C., Eds.; Elsevier: Amsterdam, 1984; Vol. 6, p 161.
(148) Hopfinger, A. J.; Pearlstein, R. A. *J. Comput. Chem.* **1984**, *5*, 486.
(149) Liljefors, T.; Allinger, N. L. *J. Comput. Chem.* **1985**, *6*, 478.
(150) Kollman, P. *Acc. Chem. Res.* **1985**, *18*, 105.
(151) Singh, U. C.; Kollman, P. A., submitted for publication in *J. Comput. Chem.*
(152) Keil, M.; Parker, G. A. *J. Chem. Phys.* **1985**, *82*, 1947.
(153) Truhlar, D. G. In *Chemical Applications of Atomic and Molecular Electrostatic Potentials*, Politzer, P., Truhlar, D. G.; Eds.; Plenum: New York, 1981; p 85.
(154) Morokuma, K.; Kitaura, K., ref 153, p 215.
(155) Kollman, P. A., ref 153, p 243.
(156) Tomasi, J., ref 153, p 257.
(157) Marcus, R. A. *J. Chem. Phys.* **1966**, *45*, 4493.
(158) Marcus, R. A. *J. Chem. Phys.* **1968**, *49*, 2610.
(159) Shavitt, I. Theoretical Chemistry Laboratory Report No. WIS-AEC-23, University of Wisconsin, 1959, unpublished.
(160) Truhlar, D. G.; Kuppermann, A. *J. Am. Chem. Soc.* **1971**, *93*, 1840.
(161) Fukui, K.; Kato, S.; Fujimoto, H. *J. Am. Chem. Soc.* **1975**, *97*, 1.
(162) Fukui, K. *Acc. Chem. Res.* **1981**, *14*, 364.
(163) Fukui, K. *Pure Appl. Chem.* **1982**, *54*, 1825.
(164) Schaefer, H. F., III. *Chem. Br.* **1975**, *11*, 227.
(165) Garrett, B. C.; Truhlar, D. G. *J. Phys. Chem.* **1982**, *86*, 1136; **1983**, *87*, 4554(E).
(166) Rai, S. N.; Truhlar, D. G. *J. Chem. Phys.* **1983**, *79*, 6046.
(167) Komornicki, A.; Ishida, K.; Morokuma, K.; Ditchfield, R.; Conrad, M. *Chem. Phys. Lett.* **1977**, *45*, 595.
(168) Halgren, T. A.; Lipscomb, W. A. *Chem. Phys. Lett.* **1977**, *49*, 225.
(169) Rothman, M. J.; Lohr, L. L., Jr. *Chem. Phys. Lett.* **1980**, *70*, 405.
(170) Pulay, P. In *The Force Concept in Chemistry*; Deb, B. M., Ed.; Van Nostrand-Reinhold: New York, 1981; p 449.
(171) Williams, I. H.; Maggiora, G. M. *J. Mol. Struct.* **1982**, *89*, 365.
(172) (a) McIver, J. W., Jr.; Komornicki, A. *Chem. Phys. Lett.* **1971**, *10*, 303. (b) Mezey, P. G.; Peterson, M. R.; Czismadia,

I. G. *Can. J. Chem.* **1977**, *55*, 2941.
(173) McIver, J. W., Jr.; Komornicki, A. *J. Am. Chem. Soc.* **1972**, *94*, 2625.
(174) Sinclair, J. E.; Fletcher, R. *J. Phys. C* **1974**, *7*, 864.
(175) Poppinger, D. *Chem. Phys. Lett.* **1975**, *34*, 332.
(176) Poppinger, D. *Chem. Phys. Lett.* **1975**, *35*, 550.
(177) Komornicki, A.; Ishida, K.; Morokuma, K.; Ditchfield, R.; Conrad, M. *Chem. Phys. Lett.* **1975**, *45*, 595.
(178) Müller, K.; Brown, L. D. *Theoret. Chim. Acta* **1979**, *53*, 75.
(179) Fletcher, R. *Practical Methods of Optimization*; Wiley: New York, 1980.
(180) Müller, K. *Angew. Chem., Int. Ed. Engl.* **1980**, *19*, 1.
(181) Cerjan, C. J.; Miller, W. H. *J. Chem. Phys.* **1981**, *75*, 2800.
(182) Schlegel, H. B. *J. Comput. Chem.* **1982**, *3*, 214.
(183) Simons, J.; Jorgensen, P.; Taylor, H.; Ozment, J. *J. Phys. Chem.* **1983**, *87*, 2745.
(184) Bell, S.; Crighton, J. S. *J. Chem. Phys.* **1984**, *80*, 2464.
(185) Banerjee, A.; Adams, N.; Simons, J.; Shepard, R. *J. Phys. Chem.* **1985**, *89*, 52.
(186) Garrett, B. C.; Truhlar, D. G. *J. Phys. Chem.* **1979**, *83*, 1052, 3058(E); **1983**, *87*, 4553(E).
(187) Kato, S.; Morokuma, K. *J. Chem. Phys.* **1980**, *73*, 3900.
(188) Miller, W. H.; Handy, N. C.; Adams, J. E. *J. Chem. Phys.* **1981**, *72*, 99.
(189) Miller, W. H. *J. Phys. Chem.* **1983**, *87*, 3811.
(190) Truhlar, D. G.; Brown, F. B.; Steckler, R.; Isaacson, A. D. In *The Theory of Chemical Reaction Dynamics*; Clary, D. C., Ed.; Reidel: Dordrecht, 1986; p 285.
(191) Pople, J. A.; Krishnan, R.; Schlegel, H. B.; Binkley, J. S. *Int. J. Quantum Chem., Quantum Chem. Symp.* **1979**, *13*, 225.
(192) Pulay, P. In *Applications of Electronic Structure Calculations*; Schaefer, H. F., III, Ed.; Plenum: New York, 1977; p 153.
(193) Kato, S.; Morokuma, K. *Chem. Phys. Lett.* **1979**, *65*, 19.
(194) Goddard, J. D.; Handy, N. C.; Schaefer, H. F., III. *J. Chem. Phys.* **1985**, *83*, 1162.
(195) Fitzgerald, G.; Schaefer, H. F., III. *J. Chem. Phys.* **1985**, *83*, 1162.
(196) Hoffmann, M. R.; Fox, D. J.; Gaw, J. F.; Osamura, Y.; Yamaguchi, Y.; Grev, R. S.; Fitzgerald, G.; Schaefer, H. F., III; Knowles, P. J.; Handy, N. C. *J. Chem. Phys.* **1984**, *80*, 2660.
(197) Brooks, B. R.; Laidig, W. D.; Saxe, P.; Goddard, J. D.; Yamaguchi, Y.; Schaefer, H. F., III. *J. Chem. Phys.* **1980**, *72*, 4652.
(198) Tachibana, A.; Yamashita, K.; Yomabe, T.; Fukui, K. *Chem. Phys. Lett.* **1978**, *59*, 255.
(199) Gaw, J. F.; Yamaguchi, Y.; Schaefer, H. F., III. *J. Chem. Phys.* **1984**, *81*, 6395.
(200) Kitaura, K.; Obara, S.; Morokuma, K. *Chem. Phys. Lett.* **1981**, *77*, 452.
(201) Shepard, R., manuscript in preparation.
(202) Ishida, K.; Morokuma, K.; Komornicki, A. *J. Chem. Phys.* **1977**, *66*, 2153.
(203) Schmidt, M. W.; Gordon, M. S.; Dupuis, M. *J. Am. Chem. Soc.* **1985**, *107*, 2585.
(204) Garrett, B. C.; Redmon, M.; Steckler, R.; Truhlar, D. G.; Gordon, M. S.; Baldridge, K. K.; Bartol, D.; Schmidt, M. W., manuscript in preparation.
(205) Truhlar, D. G. *J. Chem. Phys.* **1970**, *53*, 2041.
(206) Duff, J. W.; Truhlar, D. G. *J. Chem. Phys.* **1975**, *62*, 2477.
(207) Truhlar, D. G.; Garrett, B. C. *Acc. Chem. Res.* **1980**, *13*, 440.
(208) Tucker, S. C.; Truhlar, D. G.; Garrett, B. C.; Isaacson, A. D. *J. Chem. Phys.* **1985**, *82*, 4102.
(209) Truhlar, D. G.; Garrett, B. C. *Annu. Rev. Phys. Chem.* **1984**, *35*, 189.
(210) Truhlar, D. G.; Kilpatrick, N. J.; Garrett, B. C. *J. Chem. Phys.* **1983**, *78*, 2438.
(211) Skodje, R. T.; Truhlar, D. G.; Garrett, B. C. *J. Chem. Phys.* **1982**, *77*, 5955.
(212) Babamov, V. K.; Marcus, R. A. *J. Chem. Phys.* **1984**, *81*, 3692.
(213) Bondi, D. K.; Connor, J. N. L.; Garrett, B. C.; Truhlar, D. G. *J. Chem. Phys.* **1983**, *78*, 5981.
(214) Garrett, B. C.; Truhlar, D. G. *J. Chem. Phys.* **1983**, *79*, 4932.
(215) Garrett, B. C.; Abusalbi, N.; Kouri, D. J.; Truhlar, D. G. *J. Chem. Phys.* **1985**, *83*, 2252.
(216) Hase, W. L. In *Potential Energy Surfaces and Dynamics Calculations*; Truhlar, D. G., Ed.; Plenum: New York, 1981; p 1.
(217) Truhlar, D. G.; Hase, W. L.; Hynes, J. T. *J. Phys. Chem.* **1983**, *87*, 2664, 5523(E).
(218) Morokuma, K. In *Frontiers of Chemistry*; Laidler, K. J., Ed.; Pergamon: Oxford, 1982; p 143.
(219) Morokuma, K.; Kato, S. In *Potential Energy Surfaces and Dynamics Calculations*; Truhlar, D. G., Ed.; Plenum: New York, 1981; p 243.
(220) Morokuma, K.; Kato, S.; Kitaura, K.; Obara, S.; Ohta, K.; Hanamura, M. In *New Horizons of Quantum Chemistry*, Löwdin, P.-O., Pullman, B., Eds.; Reidel: Dordrecht, 1983; p 221.
(221) Pople, J. A.; Beveridge, D. L. *Approximate Molecular Orbital Theory*; McGraw-Hill: New York, 1970.
(222) Bingham, R. C.; Dewar, M. J. S.; Lo, D. H. *J. Am. Chem. Soc.* **1975**, *97*, 1285.
(223) Hehre, W. J.; Stewart, R. F.; Pople, J. A. *J. Chem. Phys.* **1969**, *54*, 724.
(224) Huzinaga, G.; Andzelm, J.; Klobukowski, M.; Sakai, Y.; Tatewki, H. *Gaussian Basis Sets for Molecular Calculations*; Elsevier: Amsterdam, 1984.
(225) Dunning, T. H. *J. Chem. Phys.* **1977**, *66*, 1382.
(226) Dunning, T. H.; Hay, P. J. In *Methods of Electronic Structure Theory*; Schaefer, H. F., III, Ed.; Plenum: New York, 1977, p 1.
(227) Pietro, W. J.; Francl, M. M.; Hehre, W. J.; DeFrees, D. J.; Pople, J. A.; Binkley, J. S. *J. Am. Chem. Soc.* **1982**, *104*, 5039.
(228) Ditchfield, R.; Hehre, W. J.; Pople, J. A. *J. Chem. Phys.* **1971**, *54*, 4297.
(229) Francl, M. M.; Pietro, W. J.; Hehre, W. J.; Binkley, J. S.; Gordon, M. S.; DeFrees, D. J.; Pople, J. A. *J. Chem. Phys.* **1982**, *77*, 3654.
(230) Krishnan, R.; Binkley, J. S.; Seeger, R.; Pople, J. A. *J. Chem. Phys.* **1980**, *72*, 650.
(231) Frisch, M. J.; Pople, J. A.; Binkley, J. S. *J. Chem. Phys.* **1984**, *80*, 3265.
(232) Spitznagel, G. W.; Clark, T.; Chandrasekhar, J.; Schleyer, P. v. R. *J. Comput. Chem.* **1982**, *3*, 363.
(233) Roothaan, C. C. J. *Rev. Mod. Phys.* **1951**, *23*, 69.
(234) Pople, J. A.; Nesbet, R. K. *J. Chem. Phys.* **1954**, *22*, 571.
(235) Roothaan, C. C. J. *Rev. Mod. Phys.* **1960**, *32*, 179.
(236) Binkley, J. S.; Pople, J. A.; Dobosh, P. A. *Mol. Phys.* **1974**, *28*, 1423.
(237) Davidson, E. R.; Stenkamp, L. Z. *Int. J. Quantum Chem., Quantum Chem. Symp.* **1976**, *10*, 21.
(238) Shavitt, I. In *Methods of Electronic Structure Theory*; Schaefer, H. F., III, Ed.; Plenum: New York, 1977; p 189.
(239) Hinze, J.; Roothaan, C. C. J. *Suppl. Prog. Theor. Phys.* **1967**, *40*, 37.
(240) Roos, B. O.; Taylor, P. R.; Siegbahn, P. E. M. *Chem. Phys.* **1980**, *48*, 157.
(241) Siegbahn, P.; Heiberg, A.; Boos, B.; Levy, B. *Phys. Scr.* **1980**, *21*, 323.
(242) Ruedenberg, K.; Schmidt, M. W.; Gilbert, M. M.; Elbert, S. T. *Chem. Phys.* **1982**, *71*, 41.
(243) Lam, B.; Schmidt, M. W.; Ruedenberg, K. *J. Phys. Chem.* **1985**, *89*, 2221.
(244) Davidson, E. R.; Silver, D. M. *Chem. Phys. Lett.* **1977**, *52*, 403.
(245) Schmidt, M. W.; Gordon, M. S. *Inorg. Chem.* **1986**, *25*, 248.
(246) Hay, P. J.; Dunning, T. H. *J. Chem. Phys.* **1976**, *64*, 5077.
(247) Goddard, W. A., III; Ladner, R. C. *Int. J. Quantum Chem., Quantum Chem. Symp.* **1969**, *3*, 63.
(248) Goddard, W. A., III; Dunning, T. H., Jr.; Hunt, W. J.; Hay, P. J. *Acc. Chem. Res.* **1973**, *6*, 368.
(249) Bartlett, R. J. *Annu. Rev. Phys. Chem.* **1981**, *32*, 359.
(250) DeFrees, D. J.; Raghavachari, K.; Schlegel, H. B.; Pople, J. A. *J. Am. Chem. Soc.* **1982**, *104*, 5576.
(251) Purvis, G. D.; Bartlett, R. J. *J. Chem. Phys.* **1981**, *75*, 1284.
(252) Brown, F. B.; Truhlar, D. G. *Chem. Phys. Lett.* **1985**, *117*, 307.
(253) Gordon, M. S.; Truhlar, D. G. *J. Am. Chem. Soc.*, in press.
(254) Chiles, R. A.; Dykstra, C. E. *J. Chem. Phys.* **1981**, *74*, 4544.
(255) Dykstra, C. E.; Secrest, D. *J. Chem. Phys.* **1981**, *75*, 3967.
(256) Dykstra, C. E. *J. Mol. Struct.* **1983**, *103*, 131.
(257) Jasien, P. G.; Dykstra, C. E. *J. Am. Chem. Soc.* **1985**, *107*, 1891.
(258) Bartlett, R. J.; Dykstra, C. E.; Paldus, J. In *Advanced Theories and Computational Approaches to the Electronic Structure of Molecules*; Dykstra, C. E., Ed.; Reidel: Dordrecht, 1984; p 127.
(259) Gray, S. K.; Miller, W. H.; Yamaguchi, Y.; Schaefer, H. F., III. *J. Chem. Phys.* **1980**, *73*, 2733.
(260) Redmon, L. T.; Purvis, G. D., III; Bartlett, R. J. *J. Chem. Phys.* **1980**, *72*, 986.
(261) Redmon, L. T.; Purvis, G. D., III; Bartlett, R. J. *J. Chem. Phys.* **1978**, *69*, 5386.
(262) Saxe, P.; Yamaguchi, Y.; Pulay, P.; Schaefer, H. F., III. *J. Am. Chem. Soc.* **1980**, *102*, 3718.
(263) Jaffe, R. L.; Hayes, D. M.; Morokuma, K. *J. Chem. Phys.* **1974**, *60*, 5108.
(264) Jaffe, R. L.; Morokuma, K. *J. Chem. Phys.* **1976**, *64*, 4881.
(265) Goddard, J. D.; Schaefer, H. F., III. *J. Chem. Phys.* **1979**, *70*, 5117.
(266) Miller, W. H. *J. Am. Chem. Soc.* **1979**, *101*, 6810.
(267) Yamashita, K.; Tachibana, A.; Yamabe, T.; Fukui, K. *Chem. Phys. Lett.* **1980**, *69*, 413.
(268) Yamashita, Y.; Yamabe, T.; Fukui, K. *Chem. Phys. Lett.* **1981**, *84*, 123.
(269) Gray, S. K.; Miller, W. H.; Yamaguchi, Y.; Schaefer, H. F., III. *J. Am. Chem. Soc.* **1981**, *83*, 1900.
(270) Johnston, H. S. *Gas Phase Reaction Rate Theory*; Ronald: New York, 1966.

(271) Frisch, M. J.; Binkley, J. S.; Schaefer, H. F., III. *J. Chem. Phys.* **1984**, *81*, 1882.
(272) Harding, L. B.; Wagner, A. F. *ACS Div. Fuel Chem. Preprints* **1986**, *31*(2), 65.
(273) Dunning, T. H., Jr.; Harding, L. B.; Bair, R. A.; Eades, R. A.; Shephard, R. L. *J. Phys. Chem.* **1986**, *90*, 344.
(274) Morokuma, K.; Kato, S.; Hirao, K. *J. Chem. Phys.* **1980**, *72*, 6800.
(275) Tachibana, A.; Okazaki, I.; Koizumi, M. Hori, Yamabe, T. *J. Am. Chem. Soc.* **1985**, *107*, 1190.
(276) Miller, W. H. *J. Am. Chem. Soc.* **1979**, *101*, 6810.
(277) Tachibana, A.; Fueno, F.; Yamabe, T. *J. Am. Chem. Soc.* **1986**, *108*, 4346.
(278) Osamura, Y.; Schaefer, H. F., III; Gray, S. K.; Miller, W. H. *J. Am. Chem. Soc.* **1981**, *103*, 1904.
(279) Carrington, T., Jr.; Hubbard, L. M.; Schaefer, H. F., III; Miller, W. H. *J. Chem. Phys.* **1984**, *80*, 4347.
(280) Hase, W. L.; Duchovic, R. J. *J. Chem. Phys.* **1985**, *83*, 3448.
(281) Mondro, S. L.; Linde, S. V.; Hase, W. L. *J. Chem. Phys.* **1986**, *84*, 3783.
(282) Russegger, P. *Chem. Phys.* **1978**, *34*, 329.
(283) Russegger, P. *Chem. Phys.* **1979**, *41*, 299.
(284) Russegger, P. *Chem. Phys. Lett.* **1980**, *69*, 362.
(285) Swanson, B. I.; Rafalko, J. J.; Rzepa, H. S.; Dewar, M. J. S. *J. Am. Chem. Soc.* **1977**, *99*, 7829.
(286) Machida, K.; Overend, J. *J. Chem. Phys.* **1969**, *50*, 4437.
(287) Duchovic, R. J.; Hase, W. L.; Schlegel, H. B.; Frisch, M. J.; Raghavachari, K. *Chem. Phys. Lett.* **1982**, *89*, 120.
(288) Brown, F. B.; Truhlar, D. G. *Chem. Phys. Lett.* **1985**, *113*, 441.
(289) Duchovic, R. J.; Hase, W. L. *Chem. Phys. Lett.* **1984**, *110*, 474.
(290) Truhlar, D. G.; Brown, F. B.; Schwenke, D. W.; Steckler, R.; Garrett, B. C. In *Comparison of Ab Initio Quantum Chemistry with Experiment for Small Molecules*; Barlett, R. J., Ed.; Reidel: Dordrecht, 1985; p 95.
(291) Schlegel, H. B. *J. Chem. Phys.* **1986**, *84*, 4530.
(292) Siegbahn, P. E. M. *Chem. Phys. Lett.* **1985**, *119*, 515.
(293) Wang, I. S. Y.; Karplus, M. *J. Am. Chem. Soc.* **1973**, *95*, 8160.
(294) Bauschlicher, C. W., Jr.; Haber, K.; Schaefer, H. F., III; Bender, C. F. *J. Am. Chem. Soc.* **1977**, *99*, 3610.
(295) Gordon, M. S.; Gano, D. R.; Binkley, J. S.; Frisch, M. J. *J. Am. Chem. Soc.* **1986**, *108*, 2191.
(296) Gordon, M. S.; Gano, D. R. *J. Am. Chem. Soc.* **1984**, *106*, 5421.
(297) Colwell, S. M. *Mol. Phys.* **1984**, *51*, 1217.
(298) Colwell, S. M.; Handy, N. C. *J. Chem. Phys.* **1985**, *82*, 1281.
(299) Yamashita, K.; Yamabe, T. *Int. J. Quantum Chem., Quantum Chem. Symp.* **1983**, *17*, 177.
(300) Morokuma, K.; Davis, R. E. *J. Am. Chem. Soc.* **1972**, *94*, 1060.
(301) Fukui, K.; Kato, S.; Fujimoto, H. *J. Am. Chem. Soc.* **1975**, *97*, 1.
(302) Kato, S.; Fukui, K. *J. Am. Chem. Soc.* **1976**, *98*, 6395.
(303) Truhlar, D. G.; Garrett, B. C. *Annu. Rev. Phys. Chem.* **1986**, *35*, 159.
(304) Joshi, B. D.; Morokuma, K. *J. Chem. Phys.* **1977**, *67*, 4880.
(305) Kato, S.; Morokuma, K. *J. Chem. Phys.* **1981**, *74*, 6285.
(306) Yamashita, K.; Yamabe, T.; Fukui, K. *Theor. Chim. Acta* **1982**, *60*, 523.
(307) Kato, S.; Morokuma, K. *J. Chem. Phys.* **1980**, *72*, 206.
(308) Harding, L. B. *J. Am. Chem. Soc.* **1981**, *103*, 7469.
(309) Sakai, S.; Gordon, M. S. *Chem. Phys. Lett.*, in press.
(310) Yamashita, K.; Kaminoyama, M.; Yamabe, T.; Fukui, K. *Theor. Chim. Acta* **1981**, *60*, 303.
(311) Yamabe, T.; Yamashita, K.; Kaminoyama, M.; Koizumi, M.; Tachibana, A.; Fukui, K. *J. Phys. Chem.* **1984**, *88*, 1459.
(312) Gordon, M. S.; Truhlar, D. G., unpublished results.
(313) Kato, S.; Kato, H.; Fukui, K. *J. Am. Chem. Soc.* **1977**, *99*, 684.
(314) Bicerano, J.; Schaefer, H. F., III; Miller, W. H. *J. Am. Chem. Soc.* **1983**, *105*, 2550.
(315) Carrington, T., Jr.; Miller, W. H. *J. Chem. Phys.* **1986**, *84*, 4364.
(316) Frisch, M. J.; Scheiner, A. C.; Schaefer, H. F.; Binkley, J. S. *J. Chem. Phys.* **1985**, *82*, 4194.
(317) Ohmine, I.; Morokuma, K. *J. Chem. Phys.* **1980**, *73*, 1907.
(318) Ohmine, I.; Morokuma, K. *J. Chem. Phys.* **1981**, *74*, 564.
(319) Yamabe, T.; Koizumi, M.; Yamashita, K.; Tachibana, A. *J. Am. Chem. Soc.* **1984**, *106*, 2255.